AD-A152 044 MULTI-RATE DIGITAL AUTOPILOT MODELING METHODOLOGY(U) 1/3
ARMAMENT DIV (AFSC) EGLIN AFB FL D G DIDALEUSKY MAR 85
AD-TR-83-64 AFATL-TR-83-67

UNCLASSIFIED F/G 1/3 NL

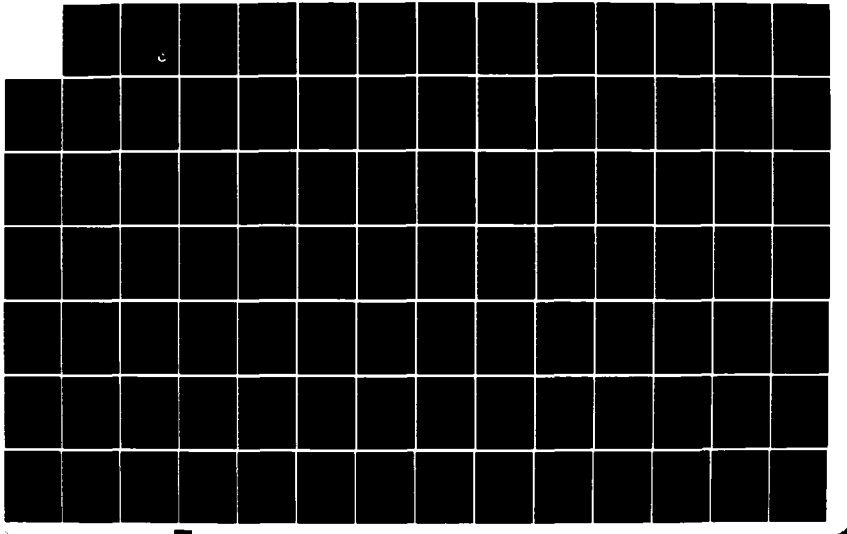

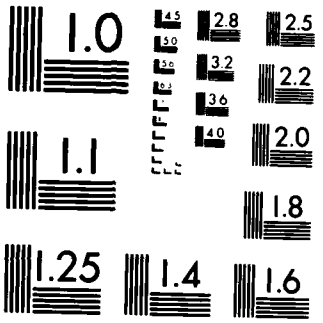

AD-TR-83-64
(AFATL-TR-83-67)

Multi-Rate Digital Autopilot Modeling Methodology

Dennis G J Didaleusky, Capt, USAF

AIR-TO-AIR SIMULATION & ANALYSIS DIVISION
DIRECTORATE OF AEROMECHANICS
DEPUTATE FOR ENGINEERING

MARCH 1985

FINAL REPORT FOR PERIOD JANUARY 1981—AUGUST 1983

Approved for public release; distribution unlimited

Armament Division
AIR FORCE SYSTEMS COMMAND★UNITED STATES AIR FORCE★EGLIN AIR FORCE BASE, FLORIDA

NOTICE

Please do not request copies of this report from the Air Force Armament Laboratory. Additional copies may be purchased from:

National Technical Information Service
5285 Port Royal Road
Springfield, Virginia 22161

Federal Government agencies and their contractors registered with Defense Technical Information Center should direct requests for copies of this report to:

Defense Technical Information Center
Cameron Station
Alexandria, Virginia 22314

UNCLASSIFIED

SECURITY CLASSIFICATION OF THIS PAGE

REPORT DOCUMENTATION PAGE

1a. REPORT SECURITY CLASSIFICATION UNCLASSIFIED	1b. RESTRICTIVE MARKINGS N/A
2a. SECURITY CLASSIFICATION AUTHORITY N/A	3. DISTRIBUTION/AVAILABILITY OF REPORT APPROVED FOR PUBLIC RELEASE; DISTRIBUTION UNLIMITED.
2b. DECLASSIFICATION/DOWNGRADING SCHEDULE N/A	
4. PERFORMING ORGANIZATION REPORT NUMBER(S) N/A	5. MONITORING ORGANIZATION REPORT NUMBER(S) AD-TR-83-64 (AFATL-TR-83-67)
6a. NAME OF PERFORMING ORGANIZATION Air-to-Air Simulation Anal Div, Dir of Aeromechanics 6b. OFFICE SYMBOL (If applicable) AD/ENMA	7a. NAME OF MONITORING ORGANIZATION N/A
6c. ADDRESS (City, State and ZIP Code) Eglin Air Force Base, Florida 32542	7b. ADDRESS (City, State and ZIP Code) N/A
8a. NAME OF FUNDING/SPONSORING ORGANIZATION Dir of Aeromech., Dep for Engrg, Armament Div 8b. OFFICE SYMBOL (If applicable) AD/ENM	9. PROCUREMENT INSTRUMENT IDENTIFICATION NUMBER In-House
8c. ADDRESS (City, State and ZIP Code) Eglin Air Force Base, Florida 32542	10. SOURCE OF FUNDING NOS. PROGRAM ELEMENT NO. 2437 / PROJECT NO. Y0 / TASK NO. 01 / WORK UNIT NO.
11. TITLE (Include Security Classification) MULTI-RATE DIGITAL AUTOPILOT MODELING METHODOLOGY	
12. PERSONAL AUTHOR(S) Dennis G. J. Didaleusky, Capt, USAF	
13a. TYPE OF REPORT Final 13b. TIME COVERED FROM Jan 81 TO Aug 83	14. DATE OF REPORT (Yr., Mo., Day) March 1985 15. PAGE COUNT 100
16. SUPPLEMENTARY NOTATION Availability of this report is specified on verso of front cover.	

17. COSATI CODES			18. SUBJECT TERMS (Continue on reverse if necessary and identify by block number)
FIELD	GROUP	SUB. GR.	Autopilot Modeling, Multi-Rate Autopilots, Multi-Rate Digital Sampling, Z-Transform Theory
01	03		
16	04	04.1	

19. ABSTRACT (Continue on reverse if necessary and identify by block number)

This technical report presents the Multi-Rate Digital Autopilot Modeling Methodology used in the analysis of guided weapon system development programs within the Armament Division. This methodology evolved from many and varied autopilot analyses and has been refined as indicated in this report. Typical guided weapon programs that have used this approach are: Advanced Medium Range Air-to-Air Missile (AMRAAM), WASP Antiarmor Missile, and Low Level Laser Guided Bomb (LLLGB). Reviews of both fundamental Z-Transform Theory and the Multi-Rate Transform are given. An example of a two-loop-per-channel autopilot typical of a symmetric missile is given. This autopilot is then modeled using Multi-Rate Transform theory to develop both open-loop and closed-loop transfer functions in the Z-plane. The computational algorithms used for Multi-Rate Modeling are referenced.

20. DISTRIBUTION/AVAILABILITY OF ABSTRACT UNCLASSIFIED/UNLIMITED ☒ SAME AS RPT. ☐ DTIC USERS ☐	21. ABSTRACT SECURITY CLASSIFICATION UNCLASSIFIED
22a. NAME OF RESPONSIBLE INDIVIDUAL Captain Joseph S. Smyth	22b. TELEPHONE NUMBER (Include Area Code) (904) 882-3053 22c. OFFICE SYMBOL AD/ENMA

DD FORM 1473, 83 APR EDITION OF 1 JAN 73 IS OBSOLETE.

UNCLASSIFIED

SECURITY CLASSIFICATION OF THIS PAGE

PREFACE

This technical report is based on work conducted by Captain Dennis G. J. Didaleusky within the Air-to-Air Simulation and Analysis Division, Aeromechanics Directorate, Deputy for Engineering, Armament Division, Eglin Air Force Base Florida 32542. The work was conducted during the period January 1981 to August 1983.

This report has been reviewed by the Public Affairs Office and is releasable to the National Technical Information Service (NTIS), where it will be available to the general public, including foreign nationals.

This technical report has been reviewed and is approved for publication.

FOR THE COMMANDER

Leroy J. Treadway

LEROY J. TREADWAY
Chief, Air-to-Air Simulation and Analysis Division
Aeromechanics Directorate

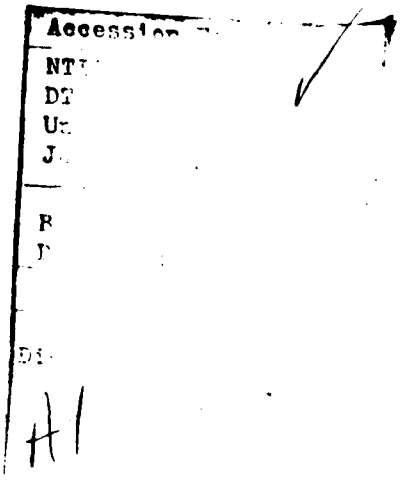

(The reverse of this page is blank)

TABLE OF CONTENTS

TABLE OF CONTENTS (CONCLUDED)

LIST OF FIGURES

LIST OF TABLES

SECTION I

INTRODUCTION

The overall function of the Multi-Rate Digital Autopilot is to provide stability augmentation for the pitch, yaw, and roll axis of an aerodynamic or space vehicle and improve dynamic response. The generic multi-rate loop structure is similar for most applications. The selection of the sampling and iteration rates is dictated by the critical performance specifications, inherent system characteristics, and design technique employed (i.e., direct digital design or emulation). Sampling here refers to the rates (i.e., samples per second) at which signals are coupled to and from the digital elements within the autopilot. The iteration rates are the rates at which the digital filters or algorithms are updated. Both these rates are commonly referred to as the sample rates for the autopilot.

The general multi-rate autopilot is a hybrid system that contains both analog and discrete elements. The analog elements include the airframe dynamics, actuators, sensors, and anti-aliasing prefilters. Discrete elements include those autopilot functions performed by the microprocessor (e.g., digital filtering and gain scheduling).

The sample rates in a missile autopilot can typically range from 10 to 600 Hz. A given missile autopilot might employ rates of 10, 20, 40, 80, and 240 Hz. These widely separated rates can significantly affect the autopilot performance and stability. These effects are further accentuated by the fact that missile autopilots are typically designed using conventional analog filters and then converted to a digital structure

using a discretization technique (e.g., Tustin transform). This approximating procedure is called emulation. Since the emulated digital autopilot only approximates the analog autopilot, emulation by itself can significantly affect performance and stability.

Before the effects of multi-rate sampling and emulation can be assessed, the multi-rate loop structure of the digital autopilot must be modeled. It is well known that conventional analog or single-rate techniques cannot fully model the multi-rate autopilot as it is actually implemented within the missile microprocessor. A comprehensive multi-rate methodology is needed that can provide a high fidelity model. This model must include the salient features of the multi-rate sampling scheme, data transfer and storage within the microprocessor, and actual digital filters implemented in the software.

This report presents a transfer function based methodology for accurately modeling and analyzing the multi-rate digital autopilot. This is a 'how to' report that offers practical techniques and procedures that can readily be applied by the control engineer. The multi-rate methodology is applied directly to a typical missile autopilot. However, this methodology is applicable to any general multi-rate control system.

The missile autopilot discussed in the report utilizes angular rate and linear acceleration feedback in the pitch and yaw axis. The pitch and yaw channels command normal and lateral missile acceleration, respectively. Both roll and roll angular rate are employed to maintain a relatively constant roll axis orientation.

The multi-rate modeling methodology formulates z-plane equations that are well suited to multi-rate linear analysis. Time-domain performance

can be assessed by applying a sampled step input to the closed-loop difference equation. Effective time constant, rise time, peak time, settling time, and percent of overshoot can be determined from the sampled response. In the frequency domain, bandwidth, steady state gain, phase margin, and gain margin are typically calculated from the multi-rate model equations.

The report is organized into five major sections and three appendices. Sections II and III review classical sampled data techniques for single-rate and multi-rate control systems. This review starts with the z-transform and progresses to multi-rate systems. Emphasis is placed on the practical application of multi-rate analysis techniques. Detailed mathematical derivations are omitted in these sections. Appropriate references are cited that cover the detailed analytical theory.

Section IV summarizes the specific multi-rate autopilot that is used throughout the report to illustrate the multi-rate modeling methodology. In Section V, the multi-rate methodology is applied to the pitch channel of the autopilot. Both open-loop and closed-loop multi-rate equations are generated. Section VI presents three computer programs that, together, can be used to numerically evaluate the multi-rate model equations. The Appendices expand the material in the report and present illustrative examples to help clarify the multi-rate methodology.

SECTION II

REVIEW OF FUNDAMENTAL z-TRANSFORM THEORY

A. INTRODUCTION

The fundamental principles of the z-transform are presented in this section (References 1 through 10). Practical z-transform theory is based on the assumption that the actual sampling operation can be modeled as the amplitude modulation of an impulse train. This central concept greatly simplifies the analysis and synthesis of sampled data, discrete, or digital systems. This view of the sampling process is valid for most practical systems and use of this theory is normally considered exact.

The multi-rate digital autopilot contains both continuous and discrete elements. The z-transform provides a unified analysis and synthesis technique for these hybrid systems. For a sampled continuous element, the z-transform can be considered as the Laplace transform of an impulse sequence (impulse train) where the area or strength of each individual impulse equals the value of the continuous time function at a particular discrete sampling instant. An alternate viewpoint is to consider the exponent in the z^{-n} delay operator as an ordering variable for a number sequence (or a sequence of discrete signal values) where the coefficient for the z^{-n} term equals the value of the number sequence (or the discrete signal) at the nth discrete time delay. This second viewpoint is exemplified by the direct modeling of the time-domain difference equation in the z-plane (see Section II-F).

In practice, to obtain a discrete z-plane model of a hybrid control system, the continuous time functions are first expressed in the s-plane

and then transformed to the z-plane using standard techniques such as partial fraction expansion coupled with table look up. A second z-transform method employs the inversion integral and contour integration (Reference 4). The partial fraction expansion approach is mechanized in the DISCRET computer program (Reference 11). Discrete functions (e.g., digital algorithms in a microprocessor) are first modeled with a difference equation and directly converted to the z-plane by substituting the appropriate z^{-n} delay operator for each term in the difference equation. During the design phase, it is the z-plane filter that is first obtained. This filter is then converted to a difference equation using the z^{-n} delay operator and subsequently implemented on a digital microprocessor.

No distinction is necessary between the z-transform function derived from a sampled continuous element and the z-transform function that models an inherently discrete element. Once discretized, all elements of a hybrid system can be treated using common analysis and design techniques. However, the standard z-transform models continuous functions at their sample points and does not provide inter-sample information. It may be necessary to investigate the inter-sample behavior of discretized continuous elements using such techniques as the advanced (or delayed) z-transform or the "continuous frequency response of a discretely excited system" (Reference 12).

B. DEFINITION OF THE z-TRANSFORM

The definition of the z-transform stems from the infinite summation

$$C^T(t) = c(0) + c(T)\ \delta(t-T) + c(2T)\ \delta(t-2T) + \ldots + c(\ )\ \delta(t-\ )$$
$$= \sum_{k=0}^{\infty} c(kT)\ \delta(t-kT) \quad , \quad k = 0, 1, 2, \ldots \qquad (1)$$

An alternate expression for Equation 1 is

$$C^T(t) = c(t) \sum_{k=0}^{\infty} \delta(t-kT)$$

$$= c(t) \quad \delta_T(t) \qquad (2)$$

The impulse train $\delta_T(t)$ represents a series of impulses of unit strength or area equally spaced in time and extending from zero to plus infinity.

In Equations 1 and 2, the sampled signal $C^T(t)$ is represented by impulses whose area or strength equals the magnitude of the continuous signal c(t) at the sampling instance t=kT. This view of the sampling process as the amplitude modulation of an impulse train $\delta_T(t)$ by the continuous signal c(t) (Figure 1) forms the mathematical basis for the z-transform. Such a viewpoint is justified if the actual time during which the sampler is closed is short compared to the time constants in the system under investigation. It is shown in Reference 5 that for a system with a single time constant tau = 1/a, the error using impulse modulation is less than 5 percent for a sampler pulse width h which is less than or equal to one-tenth of the time constant (i.e., $h/tau \leq 1/10$).

Taking the Laplace transform of the delayed functions in Equation 1 produces

$$C^T(s) = c(0) + c(T)e^{-sT} + c(2T)e^{-2sT} + \ldots = \sum_{k=0}^{\infty} c(KT)e^{-ksT} \qquad (3)$$

In general, if the Laplace transform of the continuous time function c(t) is a rational algebraic function, a closed form can be found for the infinite series representation of $C^T(s)$. The simple change of variable

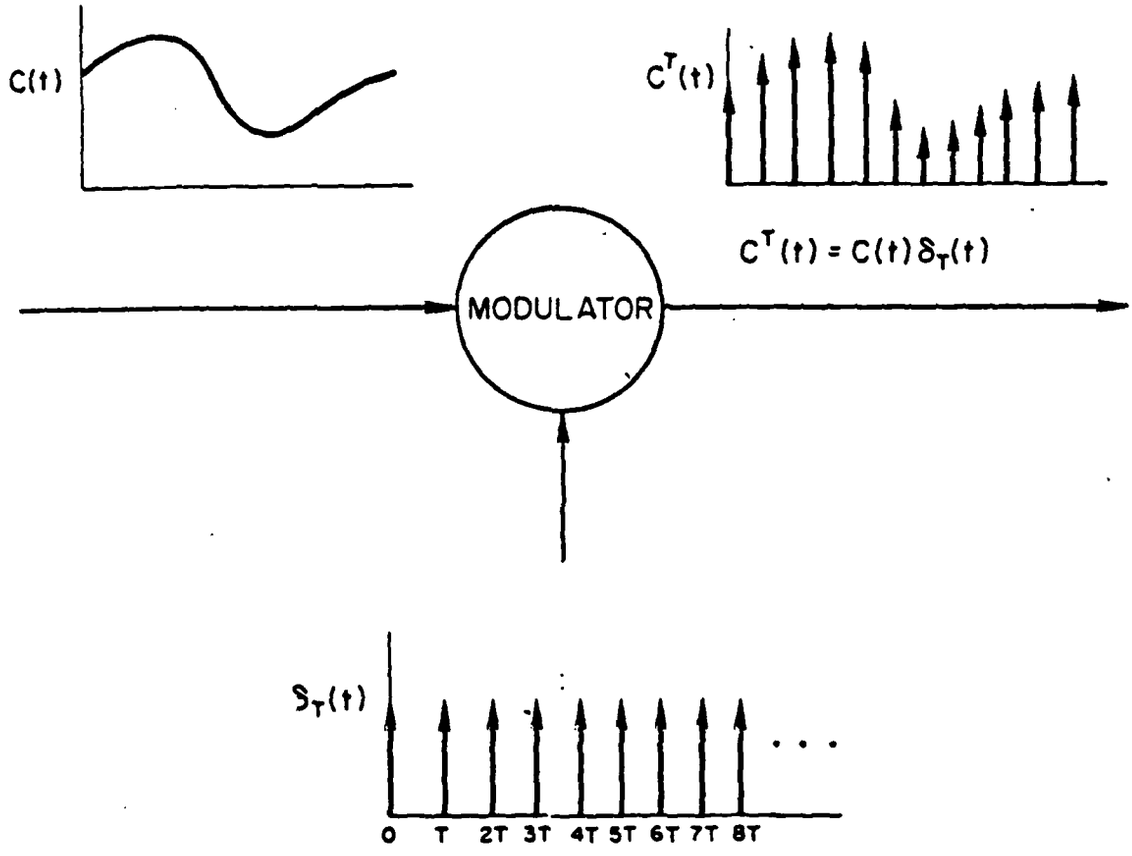

Figure 1. Amplitude Modulation of Impulse Train by Continuous Signal

$z = e^{sT}$ results in the one-sided z-transform.

$$C^T(z) = \sum_{k=0}^{\infty} c(kT)z^{-k} \tag{4}$$

For the two-sided z-transform, the lower summation limit becomes minus infinity and c(t) is defined for negative time. Most practical applications utilize the one-sided z-transform.

C. TABLE OF z-TRANSFORMS

Utilizing the fundamental definition of the z-transform in Equation 4, Reference 1 generates a table of z-transforms for elementary continuous time functions. This table is repeated here as Table 1. The column labeled $F(z, \Delta)$ is for the advanced z-transform with $0 \leq \Delta < 1$. More extensive z-transform tables can be found in References 2 through 8.

The z-transform variable in Table 1 is defined as $z = e^{sT}$, where T is the sampling interval in seconds. For other sampling intervals such as T/3, we simply replace T with T/3 in the z-transform expression. For example, consider the continuous time function $g(t) = te^{-at}$. The Laplace transform for this function is $1/(s + a)^2$ and the s-plane sampled function is given by

$$G^{T/3}(s) = \left[\frac{1}{(s + a)^2}\right]^{T/3} \tag{5}$$

The z-transform for Equation 5 can be obtained directly from Table 1.

$$G^{T/3}(z) = \frac{(T/3)ze^{-aT/3}}{(z - e^{-aT/3})^2} \tag{6}$$

where

TABLE 1. TRANSFORM TABLE

f(t)	F(s)	F(z)	F(z, Δ) = Z[f(t + ΔT)]
u(t)	$\frac{1}{s}$	$\frac{z}{z-1}$	$\frac{z}{z-1}$
t	$\frac{1}{s^2}$	$\frac{Tz}{(z-1)^2}$	$\frac{z[\Delta Tz + T(1-\Delta)]}{(z-1)^2}$
$\frac{t^2}{2}$	$\frac{1}{s^3}$	$\frac{T^2z(z+1)}{2(z-1)^3}$	$\frac{T^2z\left[\frac{\Delta^2}{2}z^2 + \left(\frac{1}{2} - \Delta^2 + \Delta\right)z + \left(\frac{1}{2} - \Delta + \frac{\Delta^2}{2}\right)\right]}{(z-1)^3}$
e^{-at}	$\frac{1}{s+a}$	$\frac{z}{z-e^{-aT}}$	$\frac{ze^{-a\Delta T}}{z-e^{-aT}}$
te^{-at}	$\frac{1}{(s+a)^2}$	$\frac{Tze^{-aT}}{(z-e^{-aT})^2}$	$\frac{ze^{-a\Delta T}[\Delta Tz + T(1-\Delta)e^{-aT}]}{(z-e^{-aT})^2}$
sin bt	$\frac{b}{s^2+b^2}$	$\frac{z \sin bT}{(z-\cos bT)^2 + (\sin bT)^2}$	$\frac{z[(\sin b\Delta T)z + \sin b(1-\Delta)T]}{z^2 - 2\cos bTz + 1}$
cos bt	$\frac{s}{s^2+b^2}$	$\frac{z(z-\cos bT)}{(z-\cos bT)^2 + (\sin bT)^2}$	$\frac{z[(\cos b\Delta T)z - \cos b(1-\Delta)T]}{z^2 - 2\cos bTz + 1}$
e^{-at} sin bt	$\frac{b}{(s+a)^2+b^2}$	$\frac{ze^{-aT}\sin bT}{(z-e^{-aT}\cos bT)^2 + (e^{-aT}\sin bT)^2}$	$\frac{ze^{-a\Delta T}[(\sin b\Delta T)z + e^{-aT}\sin b(1-\Delta)T]}{z^2 - 2e^{-aT}\cos bTz + e^{-2aT}}$
e^{-aT} cos bt	$\frac{s+a}{(s+a)^2+b^2}$	$\frac{z(z-e^{-aT}\cos bT)}{(z-e^{-aT}\cos bT)^2 + (e^{-aT}\sin bT)^2}$	$\frac{ze^{-a\Delta T}[(\cos b\Delta T)z - e^{-aT}\cos b(1-\Delta)T]}{z^2 - 2e^{-aT}\cos bTz + e^{-2aT}}$

Note: $(z - e^{-aT}\cos bT)^2 + (e^{-aT}\sin bT)^2 = z^2 - 2e^{-aT}\cos bTz + e^{-2aT}$

$$z = e^{sT/3} \tag{7}$$

or

$$G^{T/3}(z_3) = \frac{(T/3)z_3 e^{-aT/3}}{(z_3 - e^{-aT/3})2} \tag{8}$$

where

$$z_3 = e^{sT/3} \tag{9}$$

The T/3 superscript on the function $G^{T/3}(s)$ and $G^{T/3}(z)$ designates the sampling interval in seconds. The use of the superscript notation becomes necessary in multi-rate systems to separate and specify the sampling interval for each functional element. The multi-rate notation is covered in Section III.

D. PARTIAL FRACTION EXPANSION AND TABLE LOOKUP

Given a sample continuous time function expressed as a sampled s-plane transfer function (e.g., $G^T(s)$), partial fraction expansion and table lookup can be used to obtain the z-plane transfer function. The sampled system in Figure 2 will be used to illustrate this approach.

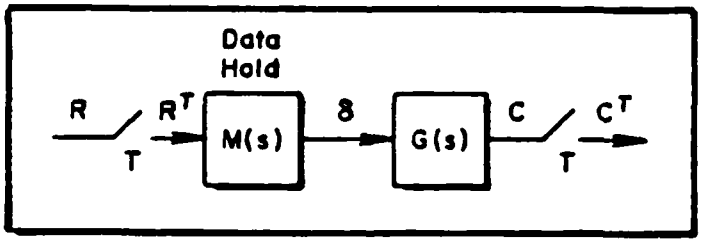

Figure 2. Typical Data Hold Configuration

The output equation for Figure 2 is given by

$$C^T = (GM)^T R^T \tag{10}$$

Let

$$M(s) = \frac{1 - e^{-sT}}{s} \quad , \quad G(s) = \frac{a}{s + a} \tag{11}$$

so that

$$(GM)^T = \left[\frac{(1 - e^{-sT})a}{s(s + a)}\right]^T = (1 - e^{-sT}) \left(\frac{1}{s} - \frac{1}{s + a}\right)^T \tag{12}$$

M(s) in Equation 11 is the s-plane transfer function for a zero-order-hold (ZOH). In Equation 12, the a/s(s + a) term is separated into two terms using partial fraction expansion (Reference 1). Since $z = e^{sT}$, $1 - e^{-sT} = 1 - z^{-1} = (z - 1)/z$ and this z-plane term can be separated from the sampling operation (see Section III-D). Therefore, from Table 1 we have

$$(GM)^T = \frac{z - 1}{z} \left(\frac{z}{z - 1} - \frac{z}{z - e^{-aT}}\right) = \frac{1 - e^{-aT}}{z - e^{-aT}} \tag{13}$$

E. THE z-TRANSFORM INVERSION INTEGRAL

The inversion integral is a closed form technique for finding the inverse z-transform (Equation 14).

$$c(kT) = \frac{1}{2\pi j} \oint_{C_1} z^{k-1} C^T(z)\, dz \tag{14}$$

Equation 14 is based on the Laurent series expansion of $F(z) = z^{k-1}C^T(z)$ about z = 0. To develop Equation 14 we first expand Equation 4, the fundamental definition of the z-transform, •

$$C^T(z) = c(0) + c(T)z^{-1} + c(2T)z^{-2} + \ldots + c(kT)z^{-k} + \ldots \tag{15}$$

If we now multiply Equation 15 by z^{k-1}, we get

$$F^T(z) = z^{k-1}C^T(z) = c(0)z^{k-1} + c(T)z^{k-2} + \ldots + c(kT)z^{-1} + \ldots \qquad (16)$$

The desired output c(kT) in the Laurent series expansion (Equation 16) is defined as the residue of the function $F^T(z)$. To obtain Equation 14 from Equation 16, we take the closed contour integral of Equation 16 and apply the Cauchy Theorem. This theorem states that if a complex integral is defined by

$$\frac{1}{2\pi j} \oint_{C_1} z^k \, dz \qquad (17)$$

and the integral is taken around a closed contour C_1 which encloses the origin of the z-plane, then the value of the integral reduces to

$$\begin{aligned} z^k dz &= 2\pi j, \text{ for } k = -1 \\ &= 0 \quad , \text{ for } k \neq -1 \end{aligned} \qquad (18)$$

Continuing with the derivation, the closed contour integral of Equation 16 is given by

$$\frac{1}{2\pi j} \oint_{C_1} z^{k-1}C^T(z)\, dz = \frac{1}{2\pi j} \oint_{C_1} C(0)z^{k-1} + \ldots + c(kT)z^{-1} + \ldots dz = c(kT) \qquad (19)$$

The right hand side of Equation 19 reduces to c(kT) since only the z^{-1} term the integration is non-zero. That is,

$$\frac{1}{2\pi j} c(kT) \oint_{C_1} z^{-1}\, dz = \frac{1}{2\pi j} c(kT)\, 2\pi j = c(kT) \qquad (20)$$

The left hand side of Equation 19 is the inversion integral given in Equation 14. Applying a second Cauchy Theorem, this integral reduces to

the evaluation of the residues of the poles associated with the integrand $z^{k-1}C^T(z)$. Equation 19 can then be expressed as

$$c(kT) = \sum \text{residues of } z^{k-1}C^T(z)\Big|_{\text{poles of } z^{k-1}C^T(z)} \tag{21}$$

Consider the following example for Equation 21. Let

$$C^T(z) = \frac{.8z}{(z - .1)\,)z - .9)} \tag{22}$$

Inserting Equation 22 into Equation 21 produces

$$c(kT) = \text{residues } z^{k-1} \left.\frac{.8z}{(z - .1)(\,z - .9)}\right|_{z = .1,\ .9}$$

$$= \left.\frac{.8z^k}{z - .1}\right|_{z = .9} + \left.\frac{.8z^k}{z - .9}\right|_{z = .1}$$

$$= (.9)^k - (.1)^k \tag{23}$$

F. SAMPLED OR DISCRETE TIME RESPONSE

The discrete time response for a z-plane transfer function can be calculated using the z-transform inversion integral (Equation 21). The use of this summation is not always practical or convenient since it requires the calculation of residues. Appendix C in Reference 1 demonstrates various techniques for obtaining the discrete time response. This subsection presents two of these techniques, the recursion or difference equation and continued fraction expansion. The single-rate sampled system in Figure 3 will be used to illustrate these two techniques.

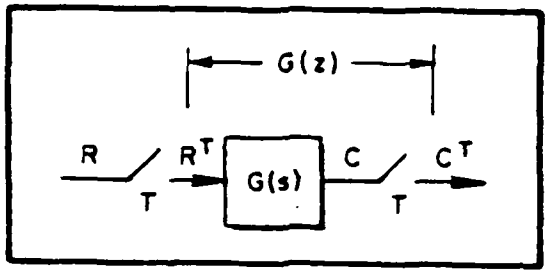

Figure 3. Single-Rate Sampled System

In the continued fraction expansion approach, the output sampled variable $C^T(z)$ is expressed as a product of the z-plane transfer function for the system and the z-plane expression for the sampled input.

$$C^T(z) = G^T(z)R^T(z) \tag{24}$$

The numerator of this z-plane product $G^T(z)R^T(z)$ is divided by the denominator and the negative powers of z^{-n} in the quotient are interpreted as impulse functions shifted in time [i.e., $z^{-n} = e^{-snT} = \delta(t-nT)$]. Suppose

$$G^T(z) = \frac{.75z}{z^2 - .75z + .125} \quad , \quad R^T(z) = 1 \tag{25}$$

Then

$$C^T(z) = G^T(z)R^T(z) = \frac{.75z}{z^2 - .75z + .125}$$

$$= .75z^{-1} + .5625z^{-2} + .328125z^{-3} + .17578125z^{-4} + \ldots \tag{26}$$

From the negative exponents in Equation 26, the sampled output is written directly as

$$[c(t)]^T = .75\ \delta(t-T) + .5625\ \delta(t-2T) + .328125\ \delta(t-3T) + \ldots \qquad (27)$$

The coefficients for the shifted impulse functions are the values of the sampled output at the sample times (Figure 4). Equation 27 represents the sampled impulse response of the system $G^T(z)$ since $R^T(z) = 1$. The z-transform of a unit impulse at time t = 0 is 1.

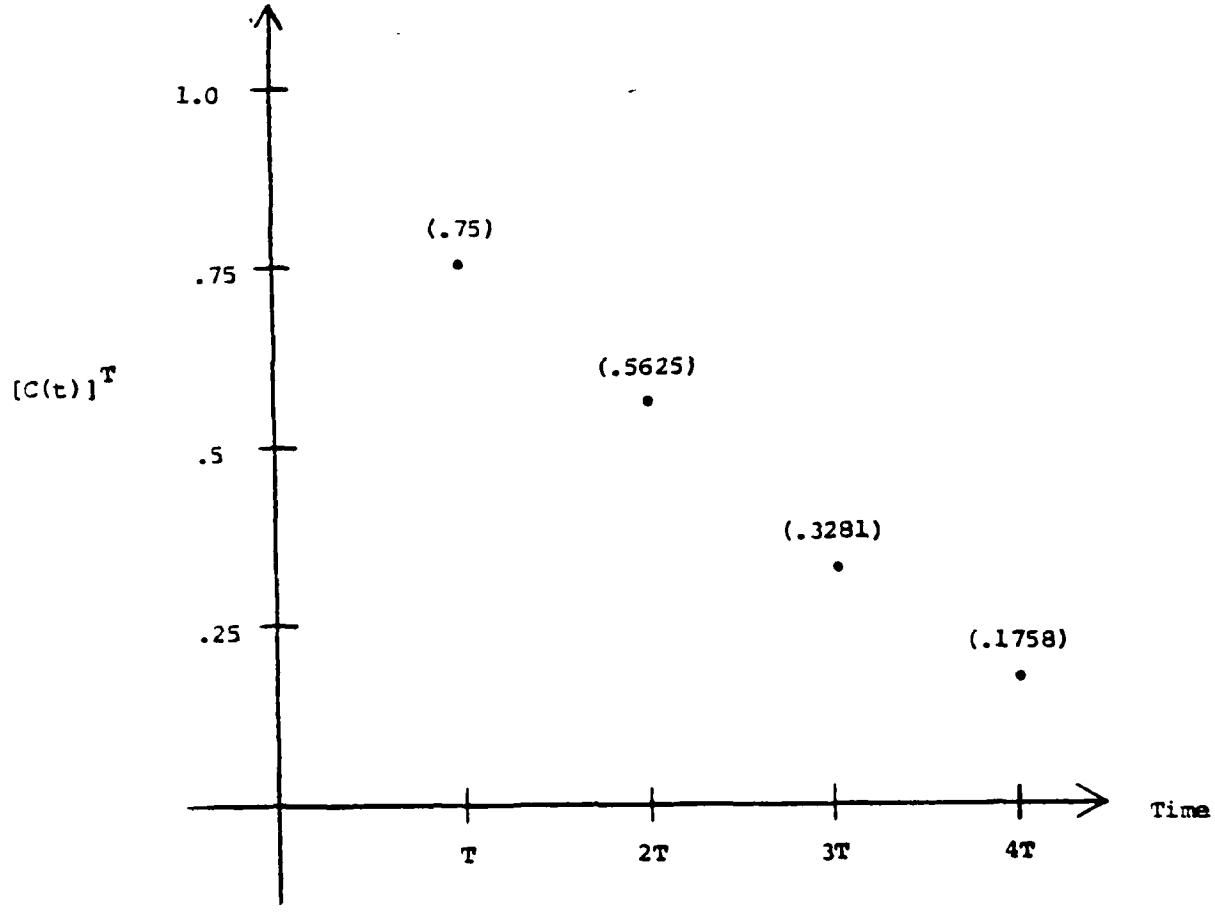

Figure 4. Discrete Time Response

Option 66 in the TOTAL computer program (Reference 13) divides polynomials and can be used to implement the continued fraction expansion technique.

The recursion or difference equation approach provides a closed form expression for the discrete time response. We first write the pulse transfer function relating the sampled output to the sampled input. For example, rewriting Equation 26 gives

$$\frac{C^T(z)}{R^T(z)} = G^T(z) = \frac{.75z}{z^2 - .75z + .125} \tag{28}$$

The pulse transfer function is next converted to negative exponent form by multiplying the numerator and denominator by z^{-n} where n is the highest power of z that appears (z^2 in Equation 28). Equation 28 then becomes

$$\frac{C^T(z)}{R^T(z)} = \frac{.75z^{-1}}{1 - .75z^{-1} + .125z^{-2}} \tag{29}$$

Cross multiplying the numerators and denominators in Equation 29 produces

$$C^T(z) \quad [1 - .75z^{-1} + .125z^{-2}] = R^T(z) \quad [.75z^{-1}] \tag{30}$$

To write the difference equation, the negative powers of z are interpreted as delayed impulse functions. That is,

$$\begin{aligned} z^{-1} &= e^{-sT} \quad \longleftrightarrow \quad \delta(t-T) \\ z^{-2} &= e^{-2sT} \quad \longleftrightarrow \quad \delta(t-2T) \\ &\vdots \\ z^{-n} &= e^{-nsT} \quad \longleftrightarrow \quad \delta(t-nT) \end{aligned} \tag{31}$$

and

$$c(kT) = .75c\,[(k-1)T] - .125c\,[(k-2)T] + .75r\,[(k-1)T] \qquad (32)$$

Equation 32 indicates that the present value of the sampled output c(kT) is a function of the past two values of the output and the past sampled value of the input. This closed form equation is calculated by Option 35 in TOTAL (Reference 13).

SECTION III

REVIEW OF THE MULTI-RATE TRANSFORM DOMAIN

A. INTRODUCTION

This section presents a brief review of the multi-rate transform domain (References 1 and 14). The major thrust to present the multi-rate notation used in the report and to summarize important multi-rate transform rules. The high-to-low rate transform conversion is also addressed along with the phantom sampler principle.

B. MULTI-RATE NOTATION

A basic multi-rate sampled system is shown in Figure 5. N is an integer so that the output sample rate is N times the input sample rate (fundamental slow input/fast output multi-rate configuration).

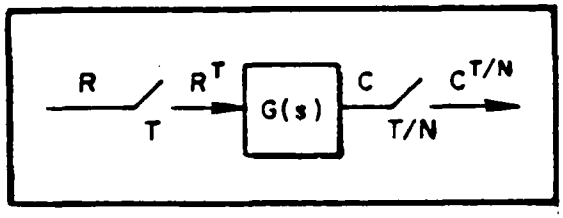

Figure 5. Multi-Rate Sampled System

The output equation for the continuous variable C is given by

$$C = GR^T \tag{33}$$

Then

$$C^{T/N} = (GR^T)^{T/N} \tag{34}$$

Since the outer sample rate operates through the inner rate (see subsection C of this section), Equation 34 reduces to

$$C^{T/N} = G^{T/N}R^{T} \tag{35}$$

The superscript notation in Equation 35 designates the time interval between each sampling operation. For example, $G^{T/N}$ indicates that the function G is sampled at N/T samples per second and R^{T} denotes that the signal R is sampled at 1/T samples per second. Also, if $G^{T/N}$ represents a digital filter implemented in a microprocessor, then T/N is the update interval of this filter in the software. These two interpretations for $G^{T/N}$ will be discussed later. The traditional notation for R^{T} and $G^{T/N}$ is $R(z)$ and $G(z_n)$, where $z = e^{sT}$ and $z_n = e^{sT/N}$. However, the superscript notation is used in the report because it permits an explicit statement of the sampling rates with minimal notational complexity.

The general notation $G^{T/N}$ implies either $G^{T/N}(s)$ or $G^{T/N}(z_n)$, they are equivalent in the discrete time domain. $G^{T/N}(s)$ represents the Laplace transform associated with the sampled continuous time function $g(kT/N)$. $G(s)$ is the Laplace transform of the continuous function $g(t)$. $G^{T/N}(s)$ is given by the standard definition of the z-transform (see Section II).

$$G^{T/N}(s) = \sum_{k=0}^{\infty} g(kT/N)e^{-ksT/N} \tag{36}$$

The equivalent $G^{T/N}(z_n)$ function is the z-transform expression obtained from $G^{T/N}(s)$ with $z_n = e^{sT/N}$. That is,

$$G^{T/N}(z_n) = G^{T/N}(s)\Big|_{z\,=\,e^{sT/N}} = \sum_{k=0}^{\infty} g(kT/N)z^{-k} \tag{37}$$

This simple change of variable ($z_n = e^{sT/N}$) converts $G^{T/N}(s)$, a nonalgebraic

function in s, to a rational function in z.

A second interpretation for the $G^{T/N}(z_n)$ function is also possible. $G^{T/N}(z_n)$ could represent the z-plane model of an inherent discrete function (e.g., digital filter implemented in a microprocessor). In this case, $G^{T/N}(z_n)$ is directly associated with a discrete time domain difference equation and is not associated with a sampled continuous time function g(kT/N) as is true in Equation 37.

To help clarify the equivalence between $G^{T/N}(s)$ and $G^{T/N}(z_n)$ and to illustrate the two possible interpretations for the z-plane function $G^{T/N}(z_n)$, consider the single rate system in Figure 6.

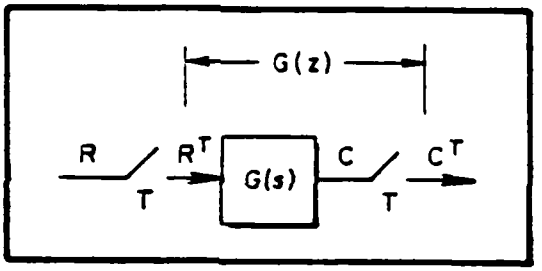

Figure 6. Single-Rate Sampled System

The output equation for Figure 6 is

$$C^T = G^T(s)R^T \tag{38}$$

Let

$$G(s) = \frac{1 - e^{-sT}}{s} \quad \frac{1}{s + 1} \tag{39}$$

Then

$$\frac{C^T}{R^T} = G^T(s) = \left(\frac{1 - e^{-sT}}{s} \quad \frac{1}{s + 1}\right)^T \tag{40}$$

Since $z = e^{sT}$,

$$G^T(s) = (1 - z^{-1}) \left(\frac{1}{s(s+1)}\right)^T$$

$$= (1 - z^{-1}) \left(\frac{1}{s} - \frac{1}{s+1}\right)^T \tag{41}$$

From the table of z-transform in Section II, the $G^T(z)$ function for Equation 41 is given by

$$G^T(z) = (1 - z^{-1}) \left(\frac{z}{z-1} - \frac{z}{z - e^{-T}}\right)$$

$$= \left(\frac{z-1}{z}\right) \frac{(1 - e^{-T})z}{(z-1)(z - e^{-T})}$$

$$= \frac{1 - e^{-T}}{z - e^{-T}} \tag{42}$$

and

$$\frac{C^T(z)}{R^T(z)} = G^T(z) = \frac{(1 - e^{-T})z^{-1}}{1 - e^{-T}z^{-1}} \tag{43}$$

The difference equation for Equation 43 is obtained by cross multiplying the numerators and denominators and interpreting z^{-1} as a one sample period delay.

$$C(kT) = e^{-T}C[(k-1)T] + (1 - e^{-T})R[(k-1)T] \tag{44}$$

Equation 44 is the difference equation for the z-plane function $G^T(z)$ in Equation 43 which is equivalent to the sampled s-plane function $G^T(s)$ in Equation 40.

A second interpretation for the general $G^T(z)$ function can be obtained from the difference equation

$$C(kT) = .9C[(k-1)T] + R(kT) + .5R[(k-1)T] \tag{45}$$

Suppose Equation 45 represents the code in a microprocessor which implements the digital filter given by

$$G^T(z) = \frac{z + .5}{z - .9} = \frac{1 + .5z^{-1}}{1 - .9z^{-1}} \tag{46}$$

In this case, the $G^T(z)$ function in Equation 46 models the discrete time domain operations in a digital microprocessor; it is not directly related to a sampled continuous function (as is true for Equation 43).

In multi-rate system design and analysis no distinction is required between the z-transform function $G^{T/N}(z)$ derived from a sampled continuous function (e.g., $G^{T/N}(s)$) and the z-transform function that models the digital operations in a microprocessor. The z-transform (and its extensions the w- or w'-transform) provides a unified analysis and synthesis technique for systems containing both continuous and discrete elements (i.e., hybrid systems). This ability to model continuous and discrete elements in a common discrete-domain is perhaps the most fundamentally useful property of the z-, w-, and w'-transforms.

C. EQUIVALENT HIGH-RATE MODEL FOR MULTI-RATE SYSTEMS

The general multi-rate transform product illustrated by Equation 35 (repeated below as Equation 47) is addressed in this subsection.

$$C^{T/N}(z_n) = G^{T/N}(z_n)R^T(z) \tag{47}$$

Equation 47 can be placed in closed form by establishing a common high-rate definition for the z-transform variable. That is,

$$C^{T/N}(z_n) = G^{T/N}(z_n)R^T(z) = G^{T/N}(z_n)R^T(z_n^N) \tag{48}$$

where

$$z = e^{sT}, \quad z_n = e^{sT/N} \tag{49}$$

To evaluate Equation 48, we first calculate the T/N and T z-transforms for $G^{T/N}(z_n)$ and $R^T(z)$, respectively. The transform variable z in $R^T(z)$ is next replaced with $z = z_n^N$. The transform product $G^{T/N}(z_n)R^T(z_n^N)$ can then be obtained since z_n appears in both functions.

Consider an example. Let

$$R(s) = \frac{1}{s} \qquad G(s) = \frac{1}{s + a} \tag{50}$$

Then

$$C^{T/N}(z_n) = \left(\frac{1}{s + a}\right)^{T/N} \left(\frac{1}{s}\right)^T \tag{51}$$

Referring to the z-transform table in Section II,

$$C^{T/N}(z_n) = \frac{z_n}{z_n - e^{-aT/N}} \quad \frac{z_n^N}{z_n^N - 1} \tag{52}$$

For N = 2 we have

$$C^{T/2}(z_2) = \frac{z_2}{z_2 - e^{-aT/2}} \quad \frac{z_2^2}{z_2^2 - 1}$$

$$= \frac{z_2^3}{(z_2 - e^{-aT/2}) \quad (z_2^2 - 1)}$$

$$= \frac{z_2^3}{z_2^3 - e^{-aT/2}z_2^2 - z_2 + e^{-aT/2}} \tag{53}$$

D. AN IMPORTANT MULTI-RATE TRANSFORM RULE

It is well-established (References 1-12) that for the single-rate system in Figure 6, the output equation is given by

$$C = GR^T \tag{54}$$

Then

$$C^T = (GR^T)^T = G^T R^T \tag{55}$$

and

$$\frac{C^T}{R^T} = G^T \tag{56}$$

or

$$\frac{C^T(z)}{R^T(z)} = G^T(z), \qquad z = e^{sT} \tag{57}$$

In Equation 57, $G^T(z)$ is defined as the pulse transfer function relating the sampled output $C^T(z)$ to the sampled input $R^T(z)$. We observe that the R^T discrete function in Equation 55 is simply separated from the resampling operation, as was done in Equation 35. These two examples illustrate a more general rule.

> The outer sampling operator $(\cdot)^{T/N}$ operates through an inner sampling operator if the ratio of the inner sampling period to the outer sampling period is an integer.

or

> If a multi-rate transform product is resampled, discrete functions within the product can be separated from the resampling operation if the resampling rate is equal to or greater than the sample rates of the individual discrete functions.

This general multi-rate transform rule is illustrated in Equation 58 (N and M are positive integers).

$$[(G_1G_2G_3 \ldots G_i)\,(R_1^T R_2^{T/2} \ldots R_n^{T/N} R_{n+1}^{T/N+1} \ldots R_{n+m}^{T/N+M})]^{T/N} =$$

$$[(G_1G_2G_3 \ldots G_i)(R_{n+1}^{T/N+1} \ldots R_{n+m}^{T/N+M})]^{T/N}\; R_1^T R_2^{T/2} \ldots R_n^{T/N} \qquad (58)$$

The $[(G_1G_2G_3 \ldots G_i)(R_{n+1}^{T/N+1} \ldots R_{n+m}^{T/N+M})]^{T/N}$ transform operation represents a high-to-low rate transform conversion since the resample rate, N/T samples per second, is lower than the inner discrete transform rates. The functions $G_1G_2G_3 \ldots G_i$ are s-plane continuous functions and $R_{n+1}^{T/N+1} \ldots R_{n+m}^{T/N+M}$ are discrete functions. (A numerical example of a high-to-low rate transform conversion is presented in Appendix B.)

An explicit example that illustrates the multi-rate transform rule in Equation 58 is given in Equation 59.

$$[G_1(s)G_2(s)G_3^T(z)G_4^{T/2}(z_2)G_5^{T/3}(z_3)G_6^{T/4}(z_4)]^{T/2} =$$

$$[G_1(s)G_2(s)G_5^{T/3}(z_3)G_6^{T/4}(z_4)]^{T/2}\; G_3^T(z)G_4^{T/2}(z_2) \qquad (59)$$

where

$$z = e^{sT}, \quad z_2 = e^{sT/2}, \quad z_3 = e^{sT/3}, \quad z_4 = e^{sT/4} \tag{60}$$

Equation 101 from Section V also applies the multi-rate transform rule in Equation 58. This example is repeated below.

$$\frac{A\hat{z}^T(z)}{A\hat{z}^T_C(z)} = \left[\frac{Az(s)}{DE} \; ACT(s)M_2(s)G_A^{T/2}(z_2)G_B^{T/2}(z_2)G_C^T(z)\right]^T$$

$$= \left[\frac{Az(s)}{DE} \; ACT(s)M_2(s)G_A^{T/2}(z_2)G_B^{T/2}(z_2)\right]^T \; G_C^T(z)$$

$$= \left[\left(\frac{Az(s)}{DE} \; ACT(s)M_2(s)\right)^{T/2} \; G_A^{T/2}(z_2)G_B^{T/2}\right]^T \; G_C^T(z) \tag{61}$$

The numerical evaluation of the high-to-low rate transform conversion in Equations 59 and 61 requires a phantom sampler and the calculation of residues. In Equation 61, the phantom sampler is used to sample the s-plane functions at a T/2 interval prior to calculating the high-to-low rate conversion. The phantom sampler principle and the high-to-low rate transform conversion are covered in the next subsections.

E. HIGH-TO-LOW RATE SAMPLING AND THE PHANTOM SAMPLER

Consider the fundamental fast-input/slow-output multi-rate sampling configuration in Figure 7. M represents the transfer function of a data hold and G a continuous system in the s-plane. In general, the output sampling interval T_2 is greater than the input sampling interval T_1; however, a direct integer ratio between output-to-input sampling is not necessarily implied. That is, T_2 is not necessarily equal to T_1 times an integer (e.g., $T_2 = 6T_1$). This simple multi-rate configuration represents a prac-

tical situation which can be analyzed using a common sampling period T such that

$$\frac{T}{M} = T_1 \qquad \frac{T}{N} = T_2 \qquad M,N = \text{integer} \tag{62}$$

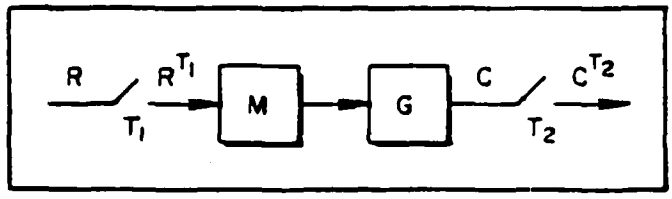

Figure 7. Fundamental Fast-Input/Slow-Output Multi-Rate Sampling, $T_2 > T_1$

For example, if the input is sampled at 20 Hz and the output at 13.33 Hz; $T_1 = 0.050$, $T_2 = 0.075$, and a choice of $T = 0.150$ produces

$$\frac{T}{3} = T_1 \qquad \frac{T}{2} = T_2 \qquad T = 0.150 \tag{63}$$

The multi-rate configuration in Figure 7 can be reduced to the general form in Figure 8.

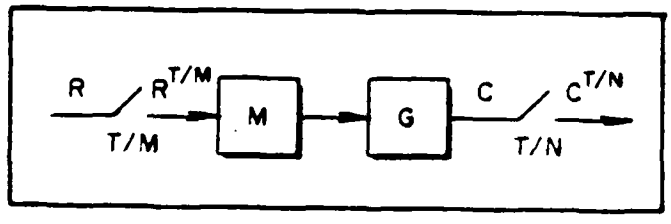

Figure 8. Fast-Input/Slow-Output Sampling with Common Sampling Period T

The output equation for Figure 8 is given by

$$C^{T/N} = [GMR^{T/M}]^{T/N} \tag{64}$$

Computationally, Equation 64 is more involved than a general slow-input/fast-output system, since the larger T/N sampling interval does not operate through the smaller T/M sampling interval (see subsection D of this section). Equation 64 can be evaluated by mathematically adding a phantom sampler to the output, Figure 9. The sample rate for the phantom sampler must be an integer multiple of the output sample rate. This mathematical trick is valid since the slower rate output sampler (N/T sampler per second) simply rejects all the unwanted samples from the higher rate phantom sampler ($1/T_*$ samples per second). With the additional phantom sampler T_*, the output equation for Figure 9 becomes

$$C^{T/N} = [(GM)^{T_*}R^{T/M}]^{T/N} \tag{65}$$

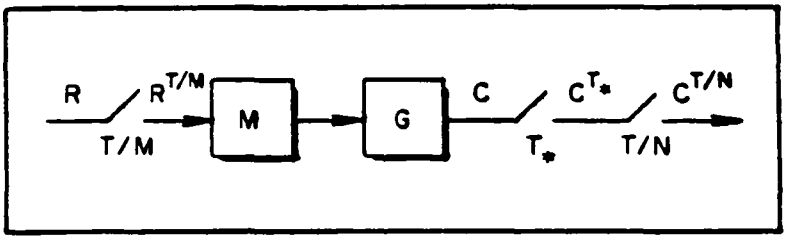

Figure 9. Fast-Input/Slow-Output Sampling with Phantom Sampler T_*

The problem now reduces to selecting T_*, calculating the transform product $GM^{T_*}R^{T/M}$, and calculating the high-to-low rate transform. As pointed out, T_* must be an integer submultiple of the output sampling interval T/N. In addition, T_* must have an integer relationship with the sampling interval T/M to allow the inner transform product to be calculated. For the most general case where M/N in Figure 9 is not an integer, an obvious choice for the phantom sampler is $T_* = T/MN$. However, if M/N is an integer, the best

choice is $T_* = T/M$. For example, if M = 3 and N = 2, $T_* = T/6$ and Equation 65 becomes

$$C^{T/2}(z_2) = [(GM)^{T/6}(z_6)R^{T/3}(z_3)]^{T/2} \tag{66}$$

Since T/6 and T/3 have an integer relationship, $z_3 = z_6^2$ and the inner transform product can be calculated using z_6 as a common variable. That is,

$$(GM)^{T/6}(z_6)R^{T/3}(z_3) = (GM)^{T/6}(z_6)R^{T/6}(z_6) = G_1^{T/6}(z_6) \tag{67}$$

where the $R^{T/6}(z_6)$ discrete function is formed by simply substituting z_6^2 for every z_3 in the $R^{T/3}(z_3)$ discrete function. Making this substitution, Equation 66 reduces to the general form

$$C^{T/2}(z_2) = [G_1^{T/6}(z_6)]^{T/2} \tag{68}$$

where

$$z_2 = e^{sT/2} \quad , \quad z_6 = e^{sT/6} \tag{69}$$

The high-to-low rate transform conversion in Equation 68 can be calculated using Equation 71 in subsection F. Note that the use of $T_* = T/MN = T/6$ has allowed the formation of the inner transform product and at the same time provided an integer ratio for the outer-to-inner sampling intervals.

F. HIGH-TO-LOW RATE TRANSFORM CONVERSION

A computer program TXCONV is presented in Reference 11 that calculates a low-rate discrete transform from a given high-rate discrete transform. The general form of this transform conversion is given by

$$C^T(z) = [C^{T/N}(z_n)]^T = [G^{T/N}R^{T/N}]^T \tag{70}$$

where

$C^T(z)$ = low-rate z-plane function, $z = e^{sT}$

$C^{T/N}(z_n)$ = high-rate z-plane function, $z_n = e^{sT/N}$

This transformation arises when a high-rate system element in a multi-rate control system is resampled at a lower rate (Figure 10). The high-to-low rate conversion in Equation 70 can be evaluated using Equation 71 (see Reference 11) for a derivation of Equation 71.

$$C^T(z) = \sum \text{residues} \quad \frac{C^{T/N}(z_n)}{z_n} \quad \frac{z}{z - z_n^N} \Bigg|_{z_n = \text{poles}} \quad \frac{C^{T/N}(z_n)}{z_n} \qquad (71)$$

The TXCONV computer program mechanizes the residue calculations in Equation 71. TXCONV is also available as options 144-149 in the TOTAL computer program (Reference 13). The user simply supplies the high-rate z-plane discrete function $G^{T/N}(z_n)R^{T/N}(z_n)$ and options 144-149 calculate the $C^T(z)$ discrete function. Appendix B presents an example in which the residue calculations in Equation 71 are illustrated.

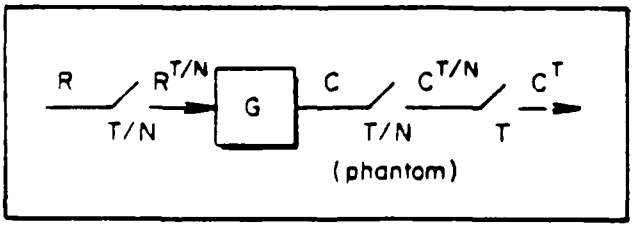

Figure 10. Fast-Input/Slow-Output Sampling with Phantom T/N Output Sampler

SECTION IV

MULTI-RATE AUTOPILOT BLOCK DIAGRAM

A. OVERALL BLOCK DIAGRAM

The block diagram in Figure 11 depicts the specific multi-rate autopilot structure used throughout the report. Angular rates (p, q, and r) and linear acceleration (Az and Ay) from body mounted sensors provide the feedback signals for the autopilot. The roll angle ϕ is obtained by integrating the output from the roll rate gyro. Angular rate feedback augments the low natural aerodynamic damping of the airframe. Acceleration feedback provides the required steady state and transient acceleration response to command inputs. Az_C and Ay_C represent command inputs to the pitch and yaw autopilot loops, respectively. The digital update rates are shown as superscripts with each digital filter. For example, the T/2 superscript indicates that the $(ATF)^{T/2}$ digital filter is updated every T/2 seconds.

$(ATF)^{T/2}$ in the autopilot is a digital notch filter that suppresses the first body bending mode of the flexible airframe. $(KTF)^{T}$ is a digital lead filter that improves the overall missile acceleration response to command inputs. ACT is the actuator transfer function, and A/C is the missile airframe transfer functions. Analog filter M_1 models the storage of data within the microprocessor. M_2 models the digital-to-analog conversion process. The remaining digital filters provide signal-conditioning (compensation) to improve missile response and stability.

B. PITCH/YAW AXIS AUTOPILOT

The autopilot in Figure 11 contains identical pitch and yaw loops

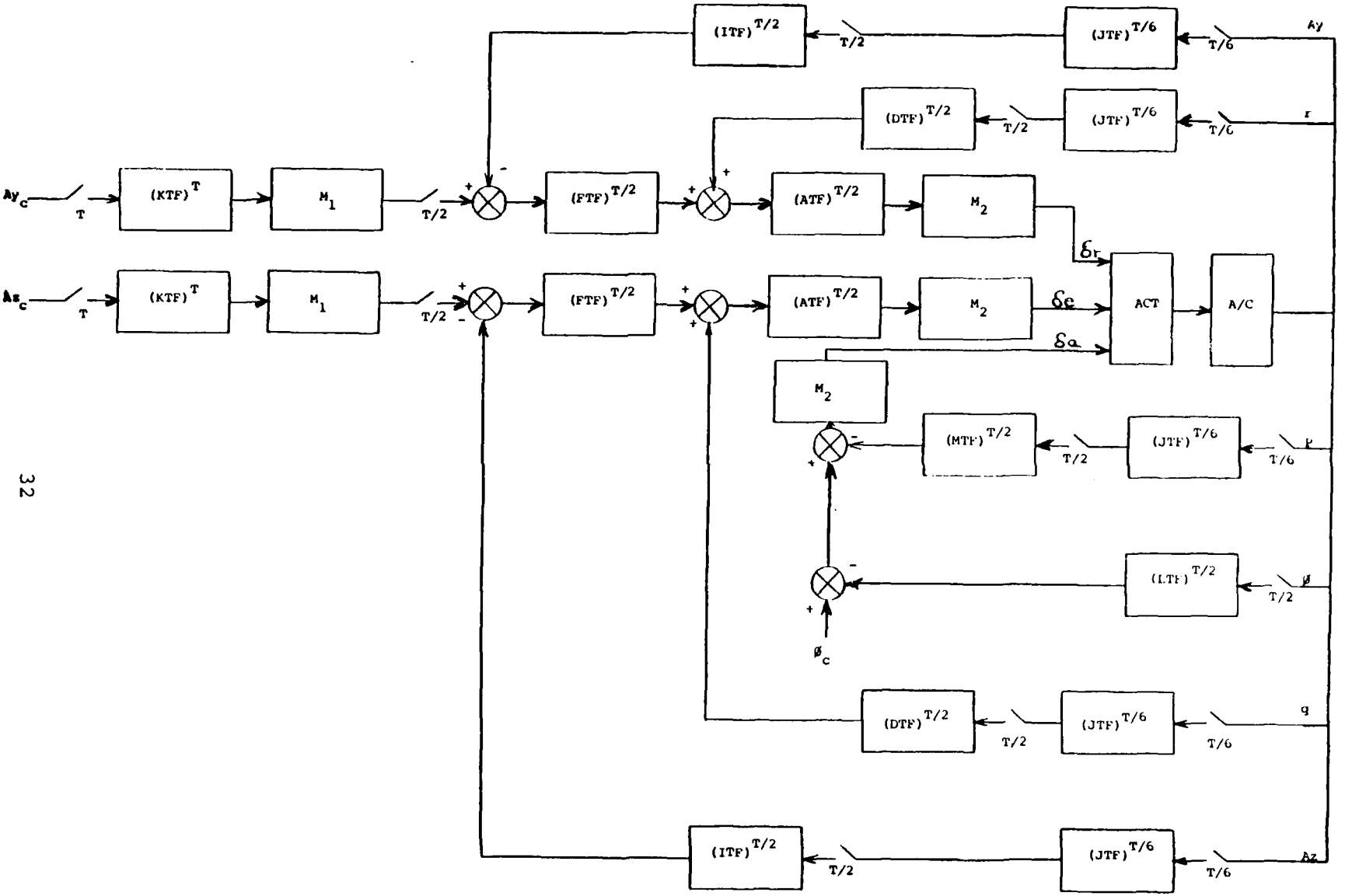

Figure 11. Typical Missile Autopilot Block Diagram

(symmetrical airframe dynamics). The pitch channel commands effective elevator deflections (δ_e) and the yaw channel rudder deflections (δ_r). In the pitch loops, body angular rate (q) about the y-axis is first sampled every T/6 seconds, averaged over three samples, resampled at a T/2 interval, and then feedback through filters $(DTF)^{T/2}$ and $(ATF)^{T/2}$. This three sample averaging is modeled with digital filter $(JTF)^{T/6}$ (see subsection IV-E). Linear acceleration (Az) along the z-axis goes through a similar T/6 sampling and averaging process and is feedback at a T/2 sampling interval through digital filters $(ITF)^{T/2}$, $(FTF)^{T/2}$, and $(ATF)^{T/2}$. This same pitch channel loop structure is used for the yaw rate (r) and y-axis linear acceleration (Ay) in the yaw autopilot loops.

C. ROLL AXIS AUTOPILOT

In the roll axis, roll rate (p) about the missile x-axis is also sampled at a T/6 interval, averaged over three samples (filter $(JTF)^{T/6}$), and feedback at a T/2 interval through digital filter $(MTF)^{T/2}$. The roll angle is feedback at a T/2 sampling interval through digital filter $(LTF)^{T/2}$. The roll autopilot provides effective aileron commands (δ_a) to the actuators.

D. ANTI-ALIASING LOW-PASS FILTERING

The analog signals from the body mounted sensors are first applied to anti-aliasing low-pass analog filters to prevent folding of the high-frequency sensor noise back into the primary frequency band of the analog-to-digital (A/D) samplers. The sensor dynamics and anti-aliasing filters are treated as unity transfer functions in the analysis and do not appear in Figure 11.

E. SENSOR THREE-SAMPLE SIGNAL AVERAGING

The output of each anti-aliasing filter is sampled at a T/6 interval. These digital signals are then averaged over three samples and feedback at a T/2 interval through the loop compensation to the servo actuators. This three sample filtering action is modeled with digital filter $(JTF)^{T/6}$.

In the discrete time domain, this filtering action is given by

$$C(kT/6) = (1/3)R(kT/6) + (1/3)R[(k-1)T/6] + (1/3)R[(k-2)T/6] \qquad (72)$$

In this difference equation, C(kT/6) is the present discrete output from the filter, and R(kT/6) is the present sampled input to the filter. R[(k-1)T/6] and R[(k-2)T/6] represent the sampled values of the input obtained during the previous two T/6 sampling times. This difference equation indicates that the present discrete output is equal to the numerical average of the present input and the previous two sampled input values.

The discrete time-domain difference equation can be modeled directly in the z-plane. The exponent on the z^{-k} delay operator is interpreted as a time domain ordering variable for each discrete signal value. The coefficient for each z^{-k} term then equals the value of the discrete signal at the kth time delay. This is the classical sampled data approach. To apply this approach, we simply associate each discrete time-domain signal value with an appropriate z^{-k} delay operator (i.e., simple substitution). Equation 72 can then be expressed as

$$C(z) = (1/3)R(z) + (1/3)z^{-1}R(z) + (1/3)z^{-2}R(z) \qquad (73)$$

For a T/6 sampling interval, the z-transform variable in Equation 73 is defined as $z = e^{sT/6}$, and z^{-1} represents a one sample period delay and

z^{-2} a two sample period delay. The $z^{-1}R(z)$ term then represents the value of the input obtained during the previous sampling time and the $z^{-2}R(z)$ term the sampled input obtained two sample periods earlier. For further insight into the meaning of the z^{-k} delay operator, see Sections II and III.

F. DIGITAL DATA STORAGE MODELING VIA ZERO-ORDER-HOLD

Since data in a multi-rate autopilot is updated at different rates and combined, the output of the filters in the slower loops must be stored in the microprocessor software between filter update times. For example, in Figure 11, the Az_c command input is sampled and filtered at a T update interval (i.e., every T seconds). This T digital signal from filter $(KTF)^T$ is combined with the T/2 digital signal from filter $(ITF)^{T/2}$ in the Az acceleration feedback loop. Since the T/2 signal arrives at the summing junction twice as often as the T sampled and filtered signal, the latest value of the T signal from filter $(KTF)^T$ must be stored in the software between the T update intervals. The alternative to this arrangement is to operate the Az_c command input in an open-loop mode every other T/2 update of filter $(ITF)^{T/2}$.

In the multi-rate autopilot, the digital storage of data between updates is modeled in the s-plane with a Zero-Order-Hold (ZOH) transfer function, M_1.

$$M_1 = \frac{1 - e^{-sT}}{s} \tag{74}$$

It is important to recognize that M_1 is not a physical ZOH hardware device (i.e., a digital-to-analog convertor). It simply models the storage of variable data within the microprocessor software between the algorithm

update times. However, the M_2 data holds in Figure 11 represent the physical ZOH hardware units that implement the digital-to-analog conversion of the signals commanding the actuators. The form of the M_2 transfer function is the same as the M_1 functional element.

$$M_2 = \frac{1 - e^{-sT/2}}{s} \tag{75}$$

G. COMMAND AUGMENTATION PREFILTER

$(KTF)^T$ in Figure 12 is a command augmentation prefilter that is used to improve the steady-state gain and dynamic response of the missile to acceleration commands (Az_c). Since this filter is outside the inner pitch loop and outer acceleration loop, it has no effect on basic missile stability.

The stability margins can be determined by opening up the inner loop at point $E^{T/2}$ in Figure 12 and calculating the open-loop z-plane transfer function. A discrete bode plot of this transfer function will reveal the gain and phase margins.

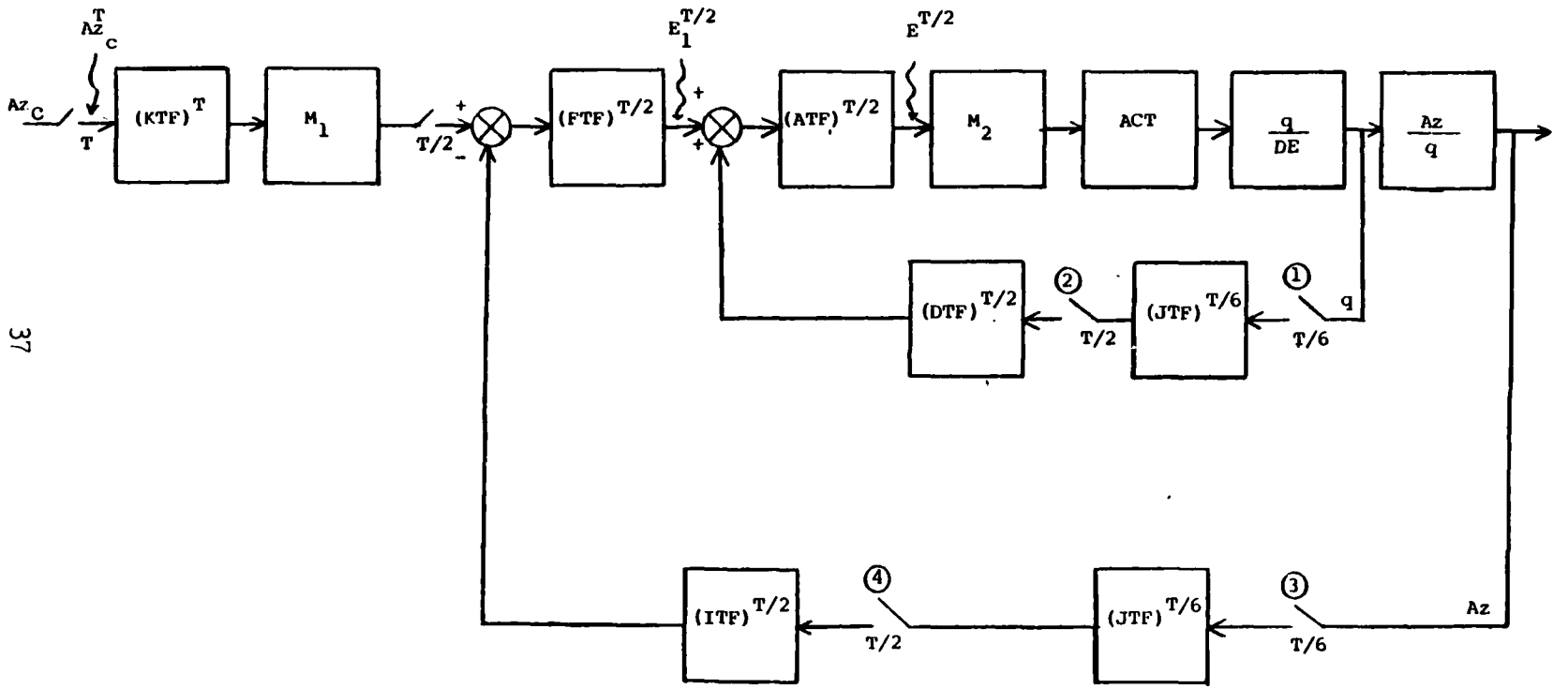

Figure 12. Pitch Channel Autopilot Block Diagram

SECTION V

MULTI-RATE MODELING METHODOLOGY

A. INTRODUCTION

The multi-rate modeling methodology presented in this section deals with the pitch channel autopilot. Since it is assumed that the pitch and yaw autopilot loops are identical (symmetrical airframe dynamics), the results in this section also apply to the yaw channel. The multi-rate equations (transfer functions) representing the pitch autopilot are formulated directly from the block diagram in Figure 12. These multi-rate equations are obtained using multi-rate block diagram algebra.

The z-plane closed-loop and open-loop transfer functions for the pitch autopilot are developed in subsections C and D, respectively. Discrete frequency and time-domain performance of the autopilot can be assessed from these transfer functions. The discrete closed-loop difference equation follows directly from the closed-loop z-plane transfer function. This difference equation quantifies the time domain performance of the autopilot (e.g., effective time constant, rise time, peak time, settling time, and percent of overshoot). To complete the analysis, closed-loop bandwidth, steady state gain, and stability margins can be determined by substituting $z = e^{jwT}$ in the z-plane transfer functions and calculating the discrete Bode plots.

B. z-PLANE PITCH AUTOPILOT BLOCK DIAGRAM

In the block diagram of the pitch autopilot, Figure 12, the third-order actuator model ACT(s) and second-order airframe transfer functions

q(s)/DE(s) and Az(s)/q(s) are expressed in the s-plane. A representative actuator model is given by

$$ACT(s) = \frac{Ka(w_a^2)p}{(s + p)(s^2 + 2\gamma_a w_a s + w_a^2)} \tag{76}$$

where γ_a is the damping ratio and w_a the undamped natural frequency of the actuator. For missile applications, (s + p) is generally a large pole (e.g., p > 100). The airframe transfer functions would appear as

$$\frac{q(s)}{DE(s)} = \frac{Kq\ (s + a)}{s^2 + 2\gamma w + w^2} \tag{77}$$

$$\frac{Az(s)}{q(s)} = \frac{Kz\ (s + b)(s + c)}{Kq\ (s + a)} \tag{78}$$

In Equation 77, γ and w represent the short period damping ratio and undamped natural frequency of the airframe, respectively. Az(s) is the acceleration along the z-axis, q(s) the pitch angular rate, and DE(s) the effective elevator deflection. The acceleration transfer function includes a nonminimum phase zero (i.e., a zero in the right-half s-plane).

The parameters for the three digital compensation filters, $(DTF)^{T/2}$, $(FTF)^{T/2}$, and $(ITF)^{T/2}$, are typically scheduled with respect to the dynamic state of the missile and/or the aerodynamic environment (e.g., Mach number, altitude, missile velocity, dynamic pressure). Representative forms for these z-plane filters can be expressed as

$$(DTF)^{T/2} = \frac{a_1 z_2 + a_2}{z_2 + a_3} \tag{79}$$

$$(FTF)^{T/2} = \frac{b_1 z_2 + b_2}{z_2 + b_3} \tag{80}$$

$$(ITF)^{T/2} = \frac{c_1 z_2 + c_2}{z_2 + c_3} \tag{81}$$

In Equations 79-81, $z_2 = e^{sT/2}$ and the a's, b's, and c's are numerical coefficients.

The digital notch filter $(ATF)^{T/2}$ is used to suppress the first body bending mode response of the missile. $(ATF)^{T/2}$ generally has a fixed structure throughout the flight envelope. This second-order z-plane filter might appear as

$$(ATF)^{T/2} = \frac{d_1 z_2^2 + d_2 z_2 + d_3}{z_2^2 + d_4 z_2 + d_5} \tag{82}$$

where $z_2 = e^{sT/2}$ and the remaining variables are numerical coefficients.

The three-sample averaging filter $(JTF)^{T/6}$ is updated every T/6 seconds. The output of this filter is sampled every T/2 seconds and feedback through the compensation in each loop. The fixed structure of this z-plane filter is given by

$$(JTF)^{T/6} = \frac{z_6^2 + z_6 + 1}{3z_6^2} \quad , \quad z_6 = e^{sT/6} \tag{83}$$

Subsection IV-E describes the function of this digital filter.

$(KTF)^T$ is a command augmentation prefilter that is used to improve the steady-state gain and dynamic response of the missile to acceleration commands (see subsection IV-6). The general form of this filter is

$$(KTF)^T = \frac{e_1 z + e_2}{z + e_3} \quad , \quad z = e^{sT} \tag{84}$$

The numerical coefficients for the $(KTF)^T$ filter are normally scheduled with respect to the dynamic state and/or aerodynamic environment of the missile.

M_1 and M_2 in Figure 12 are Zero-Order-Hold (ZOH) s-plane transfer functions expressed as

$$M_1 = \frac{1 - e^{-sT}}{s} \quad , \quad M_2 = \frac{1 - e^{-sT/2}}{s} \tag{85}$$

M_1 models the process in which the latest digital output from filter $(KTF)^T$ is stored in the microprocessor software between the T update times. The T sampled signal from $(KTF)^T$ is combined with the T/2 signal from the outer acceleration loop to form the T/2 input for filter $(FTF)^{T/2}$. As pointed out in Subsection IV-F, M_1 is not a ZOH hardware element in the autopilot. It simply models a storage process within the software. M_2, on the other hand, is a conventional ZOH hardware device that converts the digital signals from the microprocessor to analog signals for the actuators.

C. z-PLANE CLOSED-LOOP TRANSFER FUNCTION

This subsection summarizes the steps necessary to form the multi-rate closed-loop transfer function, $A_z^T/A_{z_c}^T$, for the pitch autopilot in Figure 12. This derivation is based on multi-rate block diagram algebra. For the reader who is unfamiliar with this technique, Appendix A presents a more detailed derivation of the following multi-rate equations. The following general rules of thumb are utilized in this subsection and Appendix A:

- Start at the inner loop and work outward.
- Designate the input to the inner loop data hold as a discrete

variable ($E^{T/2}$ in Figure 12)

- Designate the input to the inner loop summing junction as a discrete variable ($E_1^{T/2}$ in Figure 12)

- Designate the sampled command input as a discrete variable ($A\dot{z}_c^T$ in Figure 12)

Invoking these general rules will reduce the computations required to form the closed-loop multi-rate transfer function.

We start the derivation by writing the output equation for the inner loop continuous variable g(s) in Figure 12.

$$q(s) = \frac{q(s)}{DE(s)} ACT(s)\ M_2(s)\ E^{T/2}(z_2) \tag{86}$$

where

$$z_2 = e^{sT/2} \tag{87}$$

The T/2 superscript on the $E^{T/2}$ discrete variable designates the sampling interval in seconds. The update rate for each filter and sample rate for each signal within the autopilot block diagram will be designated using this multi-rate superscript notation (see Section III). In addition, for simplicity, the (s) and general (z) notation for each transfer function will be dropped for the remaining derivation. For example, the filter $ATF(z_2)$ is designated $(ATF)^{T/2}$, where T/2 is the sampling or update interval as reflected in the z-transform variable $z_2 = e^{sT/2}$.

Utilizing multi-rate block diagram algebra, the loop equation for the discrete variable $E^{T/2}$ can be expressed as

$$E^{T/2} = (ATF)^{T/2}E_1^{T/2} + (ATF)^{T/2}(DTF)^{T/2}\ [(JTF)^{T/6}(\frac{q}{DE}\ ACT\ M_2)^{T/6}]^{T/2}E^{T/2}$$

$$= [1 - (ATF)^{T/2}(DTF)^{T/2}[(JTF)^{T/6}(\frac{q}{DE}\ ACT\ M_2)^{T/6}]^{T/2}]^{-1}(ATF)^{T/2}E_1^{T/2}$$

$$= G_A^{T/2}E_1^{T/2} \tag{88}$$

with

$$G_A^{T/2} = [1 - (ATF)^{T/2}(DTF)^{T/2}[(JTF)^{T/6}(\frac{q}{DE}\ ACT\ M_2)^{T/6}]^{T/2}]^{-1}\ (ATF)^{T/2} \tag{89}$$

Substituting Equation 88 into Equation 86 gives the closed-loop transfer function for the inner pitch rate loop (Equation 90).

$$q = (\frac{q}{DE}\ ACT\ M_2)G_A^{T/2}E_1^{T/2} \tag{90}$$

Then

$$q = G^*E_1^{T/2} \tag{91}$$

with

$$G^* = (\frac{q}{DE}\ ACT\ M_2)G_A^{T/2} \tag{92}$$

In Equation 90, the first bracketed term on the right-hand side is a s-plane transfer function and $G_A^{T/2}$ is a z-plane transfer function. Expressing Equation 90 with more explicit notation gives

$$\frac{q(s)}{E_1^{T/2}(z_2)} = \frac{q(s)}{DE(s)}\ ACT(s)\ M_2(s)\ G_A^{T/2}(z_2) \tag{93}$$

We next write the outer loop equation for the output continuous variable Az, with the inner-pitch rate loop closed (Figure 13). This outer loop equation is given by

$$Az = (\frac{Az}{q})\ G^*E_1^{T/2} \tag{94}$$

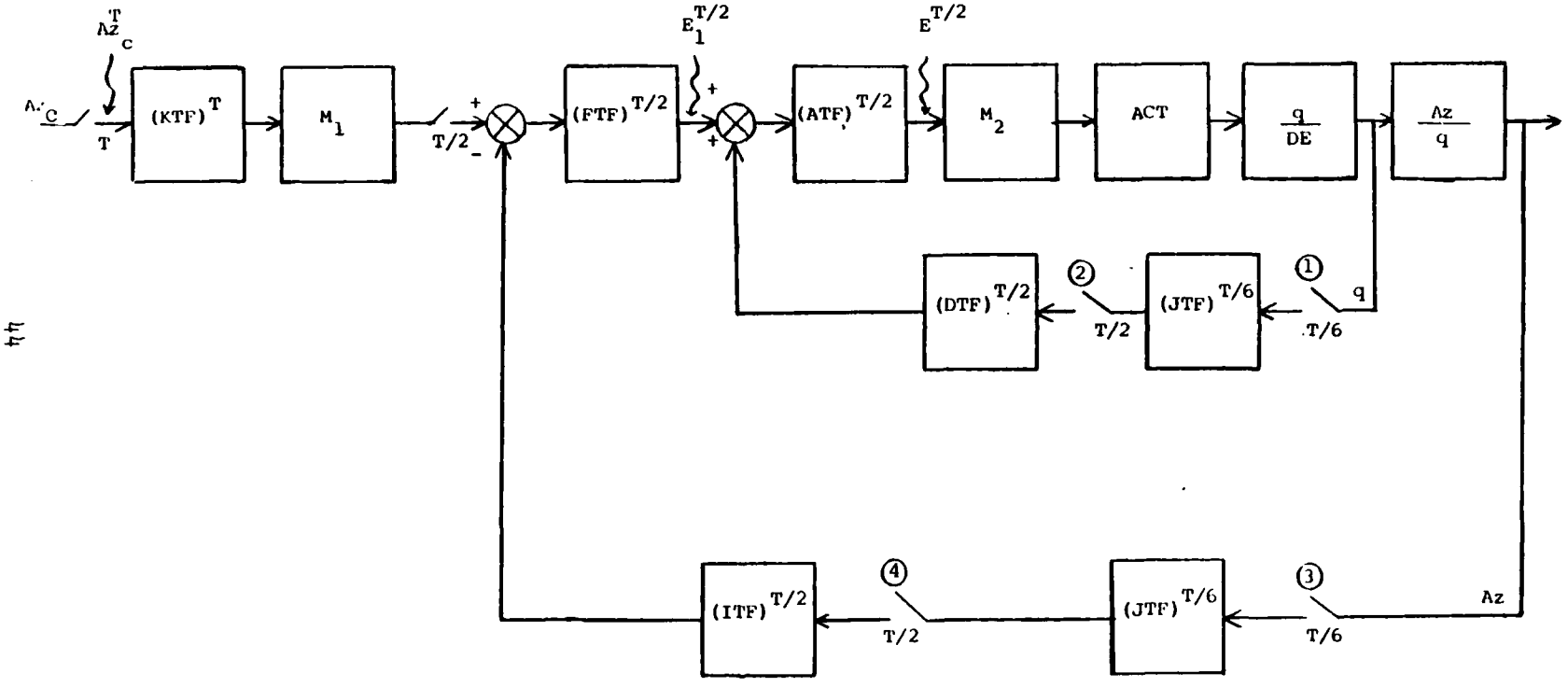

Figure 13. Pitch Channel Autopilot-Inner Rate Loop Closed

As in the inner loop, the discrete variable $E_1^{T/2}$ can be expressed as

$$E_1^{T/2} = (FTF)^{T/2} M_1^{T/2} (KTF)^T A\dot{z}_C^T - (FTF)^{T/2} (ITF)^{T/2} [(JTF)^{T/6} (\frac{Az}{q} G^*)^{T/6}]^{T/2} E_1^{T/2}$$

$$= [1 + (FTF)^{T/2} (ITF)^{T/2} [(JTF)^{T/6} (\frac{Az}{q} G^*)^{T/6}]^{T/2}]^{-1} \quad (FTF)^{T/2} M_1^{T/2} (KTF)^T A\dot{z}_C^T$$

$$= G_B^{T/2} G_C^T A\dot{z}_C^T \tag{95}$$

with

$$G_B^{T/2} = [1 + (FTF)^{T/2} (ITF)^{T/2} [(JTF)^{T/6} (\frac{Az}{q} G^*)^{T/6}]^{T/2}]^{-1} \quad (FTF)^{T/2} M_1^{T/2} \tag{96}$$

$$G_C^T = (KTF)^T \tag{97}$$

The overall closed-loop transfer function is obtained by substituting Equation 95 into Equation 94.

$$\frac{Az}{A\dot{z}_C^T} = (\frac{Az}{q} G^*) G_B^{T/2} G_C^T \tag{98}$$

Reverting back to a more explicit notation, Equation 98 becomes

$$\frac{Az(s)}{Az_C^T(s)} = \frac{Az(s)}{q(s)} \quad \frac{q(s)}{DE(s)} \; ACT(s) \; M_2(s) \quad G_A^{T/2}(z_2) G_B^{T/2}(z_2) \; G_C^T(z) \tag{99}$$

and

$$z = e^{sT} \quad , \quad z_2 = e^{sT/2} \tag{100}$$

Taking the z-transform of both sides of Equation 99 with respect to a T sampling interval produces

$$\frac{A\dot{z}^T}{A\dot{z}_C^T} = [\frac{Az}{q} \quad \frac{q}{DE} \; ACT \; M_2 \; G_A^{T/2} G_B^{T/2}]^T \quad G_C^T \tag{101}$$

Notice in Equation 101 that the bracketed factor is a high-to-low rate transform conversion and $G_A^{T/2}$ and $G_B^{T/2}$ cannot be separated from the T resampling operation (see Section III). That is,

$$\left[\frac{Az}{q}\ \frac{q}{DE}\ ACT\ M_2\ G_A^{T/2}G_B^{T/2}\right]^T \neq \left(\frac{Az}{q}\ \frac{q}{DE}\ ACT\ M_2\right)^T\ G_A^{T/2}G_B^{T/2} \qquad (102)$$

Employing the phantom sampler principle in Subsection III-E, Equation 101 can be expressed as

$$\frac{Az^T}{Az_C^T} = \left[\left(\frac{Az}{q}\ \frac{q}{DE}\ ACT\ M_2\right)^{T/2}G_A^{T/2}G_B^{T/2}\right]^T\ G_C^T \qquad (103)$$

where

$$G_A^{T/2} = \left[1 - (ATF)^{T/2}(DTF)^{T/2}\left[(JTF)^{T/6}\left(\frac{q}{DE}\ ACT\ M_2\right)^{T/6}\right]^{T/2}\right]^{-1}\ (ATF)^{T/2} \qquad (104)$$

$$G_B^{T/2} = \left[1 + (FTF)^{T/2}(ITF)^{T/2}G_A^{T/2}\left[(JTF)^{T/6}\left(\frac{Az}{DE}\ ACT\ M_2\right)^{T/6}\right]^{T/2}\right]^{-1}\ (FTF)^{T/2}M_1^{T/2} \qquad (105)$$

$$G_C^T = (KTF)^T \qquad (106)$$

Equation 103 is the z-plane closed-loop transfer function for the pitch autopilot with z defined for a 1/T sample rate (i.e., $z = e^{sT}$). A numerical example that illustrates the evaluation of Equation 103 in great detail appears in Appendix B. Also, an automated technique for evaluating Equation 103 is presented in Appendix C. This automated evaluation utilizes the macro capability of the linear analysis program TOTAL (Reference 13).

A sampled step input

$$Az_C^T = \left(\frac{1}{s}\right)^T = \frac{z}{z-1} \qquad (107)$$

can be applied to Equation 103 to determine the discrete time domain figures of merit for the pitch autopilot. Discrete time response techniques are discussed in subsection II-F.

The sampled spectrum closed-loop frequency response is obtained by evaluating Equation 103 at

$$z = e^{jwT} = 1 \angle wT \tag{108}$$

This evaluation is expressed as

$$A + jB = [(\frac{Az}{q} \quad \frac{q}{DE} \text{ ACT } M_2)^{T/2} G_A^{T/2} G_B^{T/2}]^T \; G_C^T \Big|_{z = 1\angle wT}^{z \triangleq e^{sT}} \tag{109}$$

$$= \text{Mag} \angle \phi$$

where

$$\text{Mag} = (A^2 + B^2)^{1/2} \quad , \quad \phi = \text{Tan}^{-1}(B/A) \tag{110}$$

The $z \triangleq e^{sT}$ notation in Equation 109 is for the purpose of calling out the definition of z being used in the evaluation. The complex z-plane evaluation in Equation 109 at $z = e^{jwT}$ is analogous to the classical evaluation of $s = jw$ in the s-plane. That is, at any given sinusoidal input with frequency w (see Table 1),

$$A_{Z_C}^T = (\sin wT)^T = \frac{z \sin wT}{z^2 - (2 \cos wT)z + 1} \quad , \quad z = e^{sT} \tag{111}$$

the output is also sinusoidal with frequency w, differing from the input by only a magnitude factor (Mag) and phase angle ($\angle \phi$). This represents the traditional concept of the 'sampled spectrum' which is limited to

determining the single sinusoid that fits the system output at the sample points. For a more comprehensive concept of multi-rate frequency response see References 1, 11, 12, 14, and 15. The numerical frequency evaluation given by Equation 109 is implemented as Options 50-59 and 150-159 in the linear analysis computer program TOTAL (Reference 13).

D. z-PLANE OPEN-LOOP TRANSFER FUNCTION

The open-loop transfer function for the pitch autopilot is calculated in this subsection with the loop break point at $E^{T/2}$ in Figure 12 (sometimes referred to as the servo break open-loop transfer function). At this break point, two loop paths define the open-loop z-plane transfer function. These two loops are given by

$$(OLTF)^{T/2} = (ATF)^{T/2}(FTF)^{T/2}(ITF)^{T/2}[(JTF)^{T/6}(\frac{Az}{q}\ ACT\ M_2)^{T/6}]^{T/2}$$

$$- (ATF)^{T/2}(DTF)^{T/2}[(JTF)^{T/6}(\frac{q}{DE}\ ACT\ M_2)^{T/6}]^{T/2} \qquad (112)$$

The negative sign for the second term (loop) in Equation 112 is a result of the positive sign on the inner loop summing junction.

The sampled spectrum open-loop frequency response is obtained by evaluating Equation 112 at $z = e^{jwT} = 1\angle wT$. This evaluation is expressed as

$$A + jB = G_1^{T/2} - G_2^{T/2} \Big|_{z = 1\angle wT}^{z \triangleq e^{sT/2}} \qquad (113)$$

$$= Mag\angle\phi$$

or

$$A + jB = G_3^{T/2} \Big|_{z = 1\angle wT}^{z \triangleq e^{sT/2}} \tag{114}$$

$$= \text{Mag}\angle\phi$$

where

$$\text{Mag} = (A^2 + B^2)^{1/2} \quad , \quad \phi = \text{Tan}^{-1}(B/A) \tag{115}$$

and

$$G_1^{T/2} = (ATF)^{T/2}(FTF)^{T/2}(ITF)^{T/2}\,[(JTF)^{T/6}(\tfrac{Az}{DE}\ ACT\ M_2)^{T/6}]^{T/2} \tag{116}$$

$$G_2^{T/2} = (ATF)^{T/2}(DTF)^{T/2}[(JTF)^{T/6}(\tfrac{q}{DE}\ ACT\ M_2)^{T/6}]^{T/2} \tag{117}$$

$$G_3^{T/2} = G_1^{T/2} - G_2^{T/2} \tag{118}$$

When the magnitude (Mag) and phase (ϕ) from Equation 113 or 114 are plotted with respect to frequency (w), the discrete Bode plots are obtained. These plots can be used to assess the gain and phase margins for the pitch autopilot. In the TOTAL computer program, Options 50-59 and 150-159 can be used to evaluate Equations 113 and 114.

SECTION VI

COMPUTATIONAL ALGORITHMS FOR MULTI-RATE SYSTEMS

A. INTRODUCTION

The basic problem facing the control engineer is to obtain valid discrete models of multi-rate hybrid systems (i.e., systems containing both analog and multi-rate discrete elements). These multi-rate models must be in a convenient form that can be readily analyzed using the analysis and synthesis tools available today. The preceding sections of the report presented a methodology for forming these multi-rate models. The following subsections discuss computational algorithms that are well suited for numerically evaluating these models. These algorithms are also utilized in the evaluation technique presented in Appendix C.

B. DISCRET COMPUTER PROGRAM

Once a valid multi-rate model equation is obtained, the next fundamental step is to evaluate the model and place it in a convenient transfer function form. This includes the discretization of the continuous elements in the system into a valid discrete domain. The DISCRET computer program presented in Reference 11 provides this discretization. DISCRET takes a continuous element expressed as an s-plane transfer function and transforms it into the z-, w-, or w'-plane. The program can calculate the standard, delayed, or advanced discrete transform. Data holds including the zero order, first order, second order, and slewer can be inserted into the transformation.

The discrete models of the continuous elements in the multi-rate model

equation can be readily combined with the inherent discrete elements (e.g., digital filters) to provide a unified, concise description of the system. An inherently discrete element may first be modeled with a difference equation and then directly converted to the z-plane by substituting the z^{-k} delay operator for each discrete term in the difference equation. Therefore, all the elements in the multi-rate model equation can be described by transfer functions in the z-, w-, or w'-plane. Consequently, similar frequency and time domain techniques used for continuous s-plane systems can be applied by the control system engineer to a wide variety of practical multi-rate systems.

C. TXCONV COMPUTER PROGRAM

In the multi-rate model equations, a troublesome situation arises when the digital signals are resampled at a lower rate. This sampling configuration requires the calculation of a low-rate z-plane transform from a given high-rate z-plane transfer function. The TXCONV computer program presented in Reference 11 calculates this complex transformation and makes it a routine operation in the analysis and design process. Specifically, TXCONV takes a high-rate discrete transfer function expressed in the z-, w-, or w'-plane and transforms it into a desired low-rate discrete transfer function in the z-, w-, or w'-plane.

The fundamental definition of the z-transform and the discrete inversion integral (see Section II) form the basis for the algorithms in the TXCONV computer program. The computer mechanization of the high-to-low rate transform conversion relies on the practical calculation of the residues of a complex integral. The residues for this integral are calculated in an unconventional manner using a limiting process via L'Hopital's rule. This

method simplifies the mechanization scheme and leads to a closed-form solution.

D. TOTAL COMPUTER PROGRAM

Both the DISCRET and TXCONV computer programs (Figure 14) represent essential tools for dealing with multi-rate, hybrid control systems. They provide two of the primary computational algorithms necessary to evaluate the multi-rate model equation. However, they are not the only tools or techniques required by the analyst. Other computational routines that are required include those that can manipulate and combine the polynomials and transfer functions in the multi-rate model equation. In addition, analysis algorithms are needed to calculate the root locus, frequency response, and time response in the z-, w-, or w'-plane. All these computational algorithms are available in the TOTAL computer program (Reference 13). DISCRET and TXCONV have also been integrated into TOTAL.

Over 100 options are now available to the user during the interactive execution of the TOTAL program. This interactive feature allows a close coupling between the analyst and the computing machine (digital computer), and a real-time dialog between the two can be effectively carried out. This results in a more effective and efficient usage of the computing machine and improves the accuracy and speed of the analysis and synthesis process.

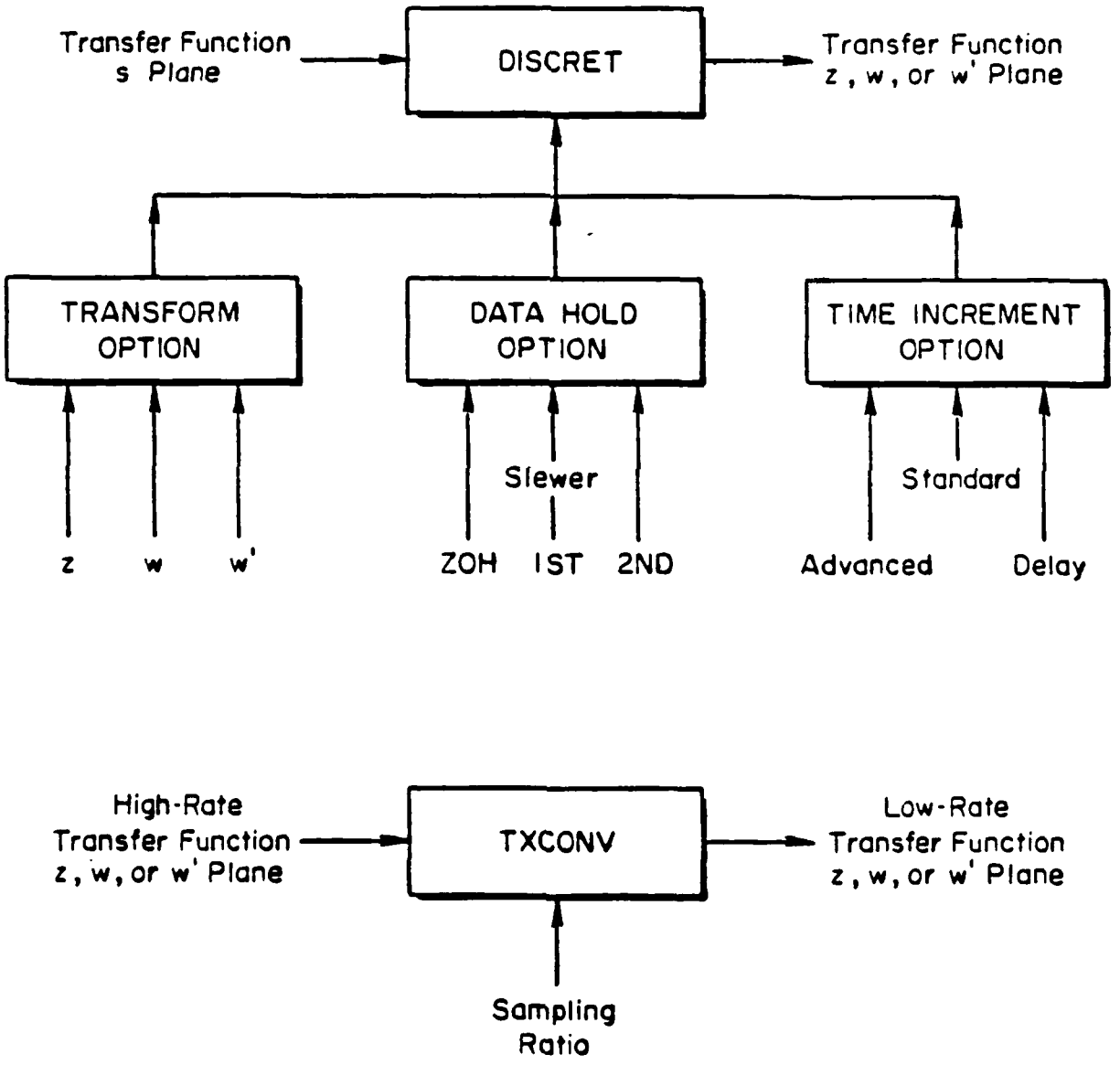

Figure 14. General Structure of DISCRET and TXCONV Computer Programs

REFERENCES

1. Whitbeck, R.F., and L.G. Hofmann, Analysis of Digital Flight Control Systems with Flying Qualities Applications, AFFDL-TR-78-115, Sept. 1978.

2. Ragazzini, J.R., and G.F. Franklin, Sampled-Data Control Systems, New York, McGraw-Hill, 1958.

3. Tou, J.T., Digital and Sampled-Data Control Systems, New York, McGraw-Hill, 1959.

4. Saucedo, R., and E.E. Schiring, Introduction to Continuous and Digital Control Systems, New York, Macmillan, 1968.

5. Jury, E.I., Sampled-Data Control Systems, New York, Wiley, 1958.

6. Jury, E.I., Theory and Application of the z-Transform Method, New York, Wiley, 1964.

7. Kuo, B.C., Analysis and Synthesis of Sampled-Data Control Systems, Englewood Cliffs, N.J., Prentice-Hall, 1963.

8. Lindorff, D.P., Theory of Sampled-Data Control Systems, New York, Wiley, 1965.

9. Kuo, B.C., Digital Control Systems, Champaign, Ill., SRL, 1977.

10. Franklin, F.F., and J.D. Powell, Digital Control of Dynamic Systems, Reading, Massachusetts, 1980.

11. Didaleusky, D.G., and R.F. Whitbeck, Multi-Rate Digital Control Systems with Simulation Applications - Volume II: Computer Algorithms, AFWAL-TR-80-3101, Sept. 1980.

12. Whitbeck, R.F., D.G. Didaleusky, and L.G. Hofmann, "Frequency Response of Digitally Controlled Systems," AIAA Journal of Guidance and Control.

13. Larimer, S.J., An Interactive Computer-Aided Design Program for Digital and Continuous Control System Analysis and Synthesis (TOTAL), AF Institute of Technology, Wright-Patterson AFB, M.S. Thesis, March 1978 (AD A055 418).

14. Whitbeck, R.F., and D.G. Didaleusky, Multi-Rate Digital Control Systems with Simulation Applications - Volume I: Technical Report, AFWAL-TR-80-3101, Sept. 1980.

15. Didaleusky, D.G., Multi-Rate Digital Control Systems with Simulation Applications - Volume III: Source Listings, AFWAL-TR-80-3101, Sept. 1980.

APPENDIX A

EXPANDED MULTI-RATE MODELING METHODOLOGY

INTRODUCTION

This appendix expands the derivation presented in Section V that leads to Equation 103. The steps in the following derivation are listed in great detail. Before proceeding, it will be helpful to review the low-to-high and high-to-low rate sampling identities. The general low-to-high rate sampling scheme is represented as (N is a positive integer)

$$[G^T(z)]^{T/N} = G^T(z) \quad , \qquad z = e^{sT} \tag{A-1}$$

However, the reverse of Equation A-1 is not true. That is,

$$[G^{T/N}(z_N)]^T \neq G^{T/N}(z_N) \quad , \qquad z_N = e^{sT/N} \tag{A-2}$$

Equation A-2 represents high-to-low rate sampling in which a high-rate sampled function $G^{T/N}(z_N)$ is resampled at a lower rate (1/T Hz). These two identities can be further expanded into the following identities:

$$[G_1(s)G_2^T(z)]^{T/N} = G_1^{T/N}(z_N)G_2^T(z) \tag{A-3}$$

$$[G_1^{T/N}(z_N)G_2^T(z)]^T = [G_1^{T/N}(z_N)]^T G_2^T(z) \tag{A-4}$$

DETAILED DERIVATION

Figure 12 from Section V is repeated here as Figure A-1. The update intervals (i.e., T, T/2, and T/6) are shown with each digital filter. The intent of the following derivation is to obtain the closed-loop z-plane transfer function given by

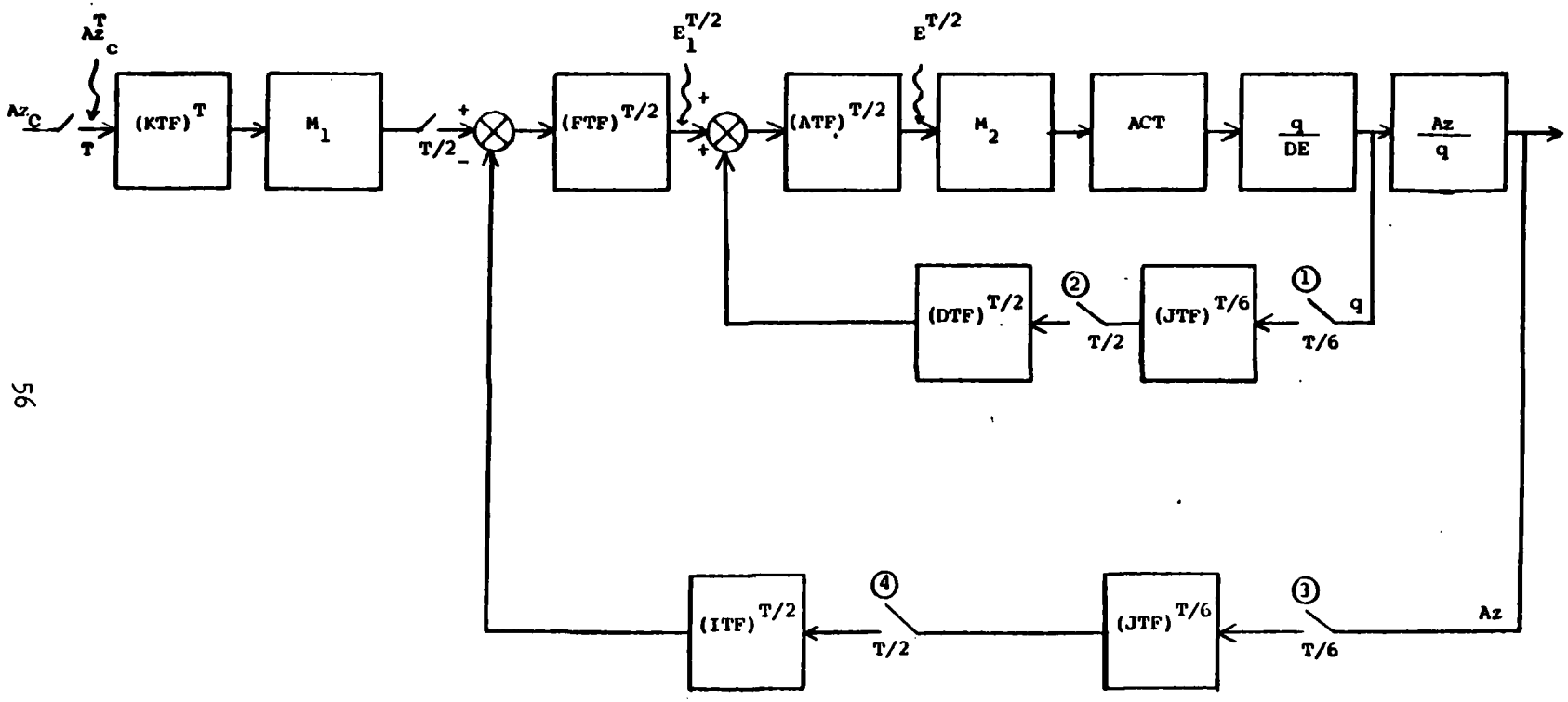

Figure A-1. Pitch Channel Autopilot Block Diagram

$$\frac{A\dot{z}^T}{A\dot{z}_C^T} = [(\frac{Az}{DE}\ ACT\ M_2)^{T/2} G_A^{T/2} G_B^{T/2}]^T\ G_C^T \qquad (A\text{-}5)$$

where

$$G_A^{T/2} = [1 - (ATF)^{T/2}(DTF)^{T/2}[(JTF)^{T/6}(\frac{q}{DE}\ ACT\ M_2)^{T/6}]^{T/2}]^{-1}\ (ATF)^{T/2} \qquad (A\text{-}6)$$

$$G_B^{T/2} = [1 + (FTF)^{T/2}(ITF)^{T/2} G_A^{T/2}[(JTF)^{T/6}(\frac{Az}{DE}\ ACT\ M_2)^{T/6}]^{T/2}]^{-1}\ (FTF)^{T/2} M_1^{T/2} \qquad (A\text{-}7)$$

$$G_C^T = (KTF)^T \qquad (A\text{-}8)$$

We start the derivation at the input to the M_2 data hold in Figure A-1. The analog pitch rate can be expressed as

$$q = \frac{q}{DE}\ ACT\ M_2\ E^{T/2} \qquad (A\text{-}9)$$

Equation A-9 indicates that the discrete signal $E^{T/2}$ is multiplied by the analog transfer functions M_2, ACT, and q/DE in order. M_2 is a Zero-Order-Hold (ZOH) that converts the discrete signal $E^{T/2}$ into an analog signal for the actuator, ACT. The airframe transfer function q/DE relates pitch rate to elevator deflection.

The discrete signal $E^{T/2}$ can be expressed as the sum of two signal paths, with one signal path being a complete loop. One signal path is associated with the discrete signal $E_1^{T/2}$ and the other with the $E^{T/2}$ signal itself. For the first signal path, the $E_1^{T/2}$ signal is simply multiplied by the $(ATF)^{T/2}$ digital filter.

$$(ATF)^{T/2} E_1^{T/2} \qquad (A\text{-}10)$$

In the second signal path which forms a complete loop, the $E^{T/2}$ signal is first multiplied by M_2, ACT, and q/DE.

$$\frac{q}{DE} \text{ ACT } M_2 E^{T/2} \tag{A-11}$$

The product in Equation A-11 is next sampled every T/6 seconds by sampler No. 1.

$$[\frac{q}{DE} \text{ ACT } M_2 E^{T/2}]^{T/6} \tag{A-12}$$

Utilizing Equation A-3, Equation A-12 reduces to

$$[\frac{q}{DE} \text{ ACT } M_2 \ E^{T/2}]^{T/6} = [\frac{q}{DE} \text{ ACT } M_2]^{T/6} \ E^{T/2} \tag{A-13}$$

The product in Equation A-13 is then multiplied by digital filter $(JTF)^{T/6}$ and resampled at a T/2 interval with sampler No. 2. These operations are expressed as

$$[(JTF)^{T/6}(\frac{q}{DE} \text{ ACT } M_2)^{T/6} E^{T/2}]^{T/2} \tag{A-14}$$

The lower rate sampled signal $E^{T/2}$ can be pulled out of the bracket in Equation A-14 (see Equation A-4). However, since we are resampling the remaining high-rate factors at a lower rate (i.e., at 2/T Hz), Equation A-14 becomes

$$[(JTF)^{T/6}(\frac{q}{DE} \text{ ACT } M_2)^{T/6} E^{T/2}]^{T/2} = [(JTF)^{T/6}(\frac{q}{DE} \text{ ACT } M_2)^{T/6}]^{T/2} \ E^{T/2} \tag{A-15}$$

When Equation A-15 is evaluated, the high-to-low rate transform will be numerically calculated. For now, we simply carry along this bracketed factor. To complete the loop, the product in Equation A-15 is multiplied by

digital filters $(DTF)^{T/2}$ and $(ATF)^{T/2}$.

$$(ATF)^{T/2}(DTF)^{T/2}[(JTF)^{T/6}(\frac{q}{DE} \text{ ACT } M_2)^{T/6}]^{T/2} \; E^{T/2} \qquad \text{(A-16)}$$

Summing Equation A-10 and Equation A-16, the $E^{T/2}$ sampled signal is given by

$$E^{T/2} = (ATF)^{T/2} \; E_1^{T/2} + (ATF)^{T/2})(DTF)^{T/2}[(JTF)^{T/6}(\frac{q}{DE} \text{ ACT } M_2)^{T/6}]^{T/2} \; E^{T/2} \qquad \text{(A-17)}$$

To solve for $E^{T/2}$, we first collect terms on the left hand side of the equation.

$$[1 - (ATF)^{T/2}(DTF)^{T/2}[(JTF)^{T/6}(\frac{q}{DE} \text{ ACT } M_2)^{T/6}]^{T/2}]E^{T/2} = (ATF)^{T/2}E_1^{T/2} \qquad \text{(A-18)}$$

Multiplying both sides of Equation A-18 by the inverse produces

$$E^{T/2} = [1 - (ATF)^{T/2}(DTF)^{T/2}[(JTF)^{T/6}(\frac{q}{DE} \text{ ACT } M_2)^{T/6}]^{T/2}]^{-1} \; (ATF)^{T/2}E_1^{T/2} \qquad \text{(A-19)}$$

Let

$$G_A^{T/2} = [1 - (ATF)^{T/2}(DTF)^{T/2}[(JTF)^{T/6}(\frac{q}{DE} \text{ ACT } M_2)^{T/6}]^{T/2}]^{-1} \; (ATF)^{T/2} \qquad \text{(A-20)}$$

Then

$$E^{T/2} = G_A^{T/2}E_1^{T/2} \qquad \text{(A-21)}$$

Substituting Equation A-21 into Equation A-9 gives

$$q = \frac{q}{DE} \text{ ACT } M_2 \; G_A^{T/2}E_1^{T/2} \qquad \text{(A-22)}$$

If we next let

$$G^* = \frac{q}{DE} \text{ ACT } M_2 \; G_A^{T/2} \tag{A-23}$$

Equation A-22 then becomes

$$q = G^* E_1^{T/2} \tag{A-24}$$

As pointed out in Section V, G^* is a hybrid function, that is, it contains both analog and discrete factors. The $\frac{q}{DE}$ ACT M_2 product results in a s-plane transfer function and $G_A^{T/2}$ is a z-plane transfer function with $z = e^{sT/2}$. Utilizing Equation A-24, we can redraw Figure A-1 as Figure A-2.

The next major step in the derivation is the closing of the outer acceleration loop. From Figure A-2, the analog normal acceleration is given by

$$Az = \frac{Az}{q} G^* E_1^{T/2} \tag{A-25}$$

Similar to $E^{T/2}$, the discrete signal $E_1^{T/2}$ can be expressed as the sum of two signal paths, with one signal path being a complete loop. The first signal path is associated with the sampled command input $A\dot{z}_c^T$ and the second with $E_1^{T/2}$ itself. The first signal path is given by

$$(FTF)^{T/2}[M_1(KTF)^T A\dot{z}_c^T]^{T/2} \tag{A-26}$$

In Equation A-26 the $A\dot{z}_c^T$ sampled signal is first multiplied by $(KTF)^T$ and M_1. This product is resampled at a T/2 interval and then multiplied by digital filter $(FTF)^{T/2}$. Since this resampling is at a higher rate, Equation A-26 reduces to (see Equation A-3)

$$(FTF)^{T/2} M_1^{T/2} (KTF)^T A\dot{z}_c^T \tag{A-27}$$

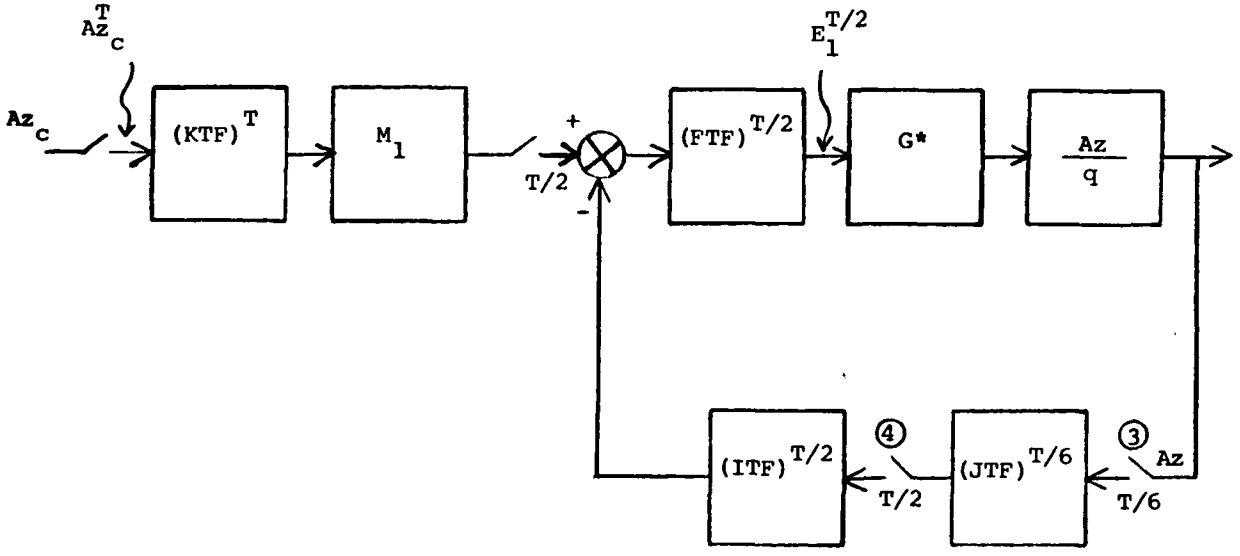

Figure A-2. Pitch Channel Autopilot - Inner Rate Loop Closed

The second signal path associated with $E_1^{T/2}$ is obtained by tracing completely around the outer acceleration loop. The $E_1^{T/2}$ discrete signal is first multiplied by the G^* and Az/q transfer functions.

$$\frac{Az}{q} G^* E_1^{T/2} \tag{A-28}$$

This product, representing the signal at the output of the Az/q block in Figure A-2, is next sampled with a T/6 interval (sampler No. 3).

$$[\frac{Az}{q} G^* E_1^{T/2}]^{T/6} \tag{A-29}$$

In Equation A-29, the $E_1^{T/2}$ signal can be pulled out since we are resampling at a higher rate (i.e., 6/T Hz).

$$(\frac{Az}{q} G^*)^{T/6} E_1^{T/2} \tag{A-30}$$

The product in Equation A-30 is multiplied by digital filter $(JTF)^{T/6}$ and the results is resampled every T/2 seconds (sampler No. 4).

$$[(JTF)^{T/6}(\frac{Az}{q} G^*)^{T/6} E_1^{T/2}]^{T/2} \tag{A-31}$$

Pulling the $E_1^{T/2}$ signal out, Equation A-31 becomes

$$[(JTF)^{T/6}(\frac{Az}{q} G^*)^{T/6}]^{T/2} E_1^{T/2} \tag{A-32}$$

The bracketed factor in Equation A-32 is a high-to-low rate conversion which must be numerically calculated (as is also true for Equation A-15). The final step for this signal path is the multiplication by digital filters $(ITF)^{T/2}$ and $(FTF)^{T/2}$.

$$(FTF)^{T/2}(ITF)^{T/2}[(JTF)^{T/6}(\frac{Az}{q}\ G^*)^{T/6}]^{T/2}E_1^{T/2} \qquad \text{(A-33)}$$

Combining the two signal path Equations A-27 and A-33 produces

$$E_1^{T/2} = (FTF)^{T/2}M_1^{T/2}(KTF)^T A\overset{T}{z}_C - (FTF)^{T/2}(ITF)^{T/2}[(JTF)^{T/6}(\frac{Az}{q}\ G^*)^{T/6}]^{T/2}E_1^{T/2} \qquad \text{(A-34)}$$

Solving for $E_1^{T/2}$ gives

$$E_1^{T/2} = [1 + (FTF)^{T/2}(ITF)^{T/2}[(JTF)^{T/6}(\frac{Az}{q}\ G^*)^{T/6}]^{T/2}]^{-1}\ (FTF)^{T/2}M_1^{T/2}(KTF)^T A\overset{T}{z}_C \qquad \text{(A-35)}$$

If we let

$$G_B^{T/2} = [1 + (FTF)^{T/2}(ITF)^{T/2}[(JTF)^{T/6}(\frac{Az}{q}\ G^*)^{T/6}]^{T/2}]^{-1}\ (FTF)^{T/2}M_1^{T/2} \qquad \text{(A-36)}$$

$$G_C^T = (KTF)^T \qquad \text{(A-37)}$$

Then

$$E_1^{T/2} = G_B^{T/2}G_C^T A\overset{T}{z}_C \qquad \text{(A-38)}$$

The overall closed loop transfer function is obtained by substituting Equation A-38 into Equation A-25.

$$Az = \frac{Az}{q}\ G^* G_B^{T/2}G_C^T A\overset{T}{z}_C \qquad \text{(A-39)}$$

We next take the z-transform of both sides of Equation A-39 with respect to a T sampling interval ($z = e^{sT}$).

$$A\overset{T}{z} = (\frac{Az}{q}\ G^* G_B^{T/2}G_C^T A\overset{T}{z}_C)^T \qquad \text{(A-40)}$$

The T transform factors can be pulled out and Equation A-40 becomes

$$\frac{A\hat{z}^T}{A\hat{z}_C^T} = \left(\frac{Az}{q}\, G^* G_B^{T/2}\right)^T G_C^T \qquad \text{(A-41)}$$

Substituting for G^* (Equation A-23), Equation A-41 can be expressed as

$$\frac{A\hat{z}^T}{A\hat{z}_C^T} = \left(\frac{Az}{DE}\, ACT\, M_2\, G_A^{T/2} G_B^{T/2}\right)^T G_C^T \qquad \text{(A-42)}$$

The final step in the derivation is to introduce a phantom T/2 sampler to Equation A-42. This mathematical operation is depicted in Figure A-3. This step is valid since the T output sampler simply rejects all the unwanted samples from the T/2 phantom sampler. Equation A-42 then becomes

$$\frac{A\hat{z}^T}{A\hat{z}_C^T} = \left[\left(\frac{Az}{DE}\, ACT\, M_2\right)^{T/2} G_A^{T/2} G_B^{T/2}\right]^T G_C^T \qquad \text{(A-43)}$$

Equation A-43 is the final result, the closed-loop z-plane transfer function for Figure A-1 ($z = e^{sT}$). The intermediate transfer function products $G_A^{T/2}$, $G_B^{T/2}$, and G_C^T are given by Equations A-20, A-36, and A-37, respectively.

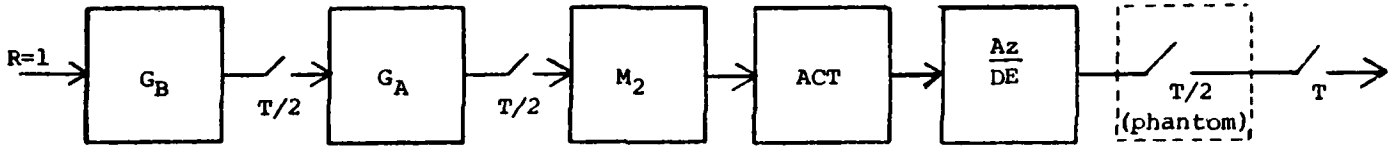

$$\left[\frac{Az}{DE}\ ACT\ M_2\ G_A{}^{T/2} G_B{}^{T/2}\right]^T = \left[\left(\frac{Az}{DE}\ ACT\ M_2\right)^{T/2} G_A{}^{T/2} G_B{}^{T/2}\right]^T$$

Figure A-3. Phantom Sampler Principle

APPENDIX B

NUMERICAL EVALUATION OF MULTI-RATE MODEL EQUATIONS

INTRODUCTION

This appendix outlines the step-by-step procedures for numerically evaluating the z-plane closed-loop transfer function expressed in Equations 103-106, Section V. This multi-rate equation is repeated below.

$$\frac{\overset{T}{Az}}{\overset{T}{Az}_C} = [(\frac{Az}{DE}\ ACT\ M_2)^{T/2} G_A^{T/2} G_B^{T/2}]^T\ G_C^T \qquad (B\text{-}1)$$

$$G_A^{T/2} = [1 - (ATF)^{T/2}(DTF)^{T/2}[(JTF)^{T/6}(\frac{q}{DE}\ ACT\ M_2)^{T/6}]^{T/2}]^{-1}(ATF)^{T/2} \qquad (B\text{-}2)$$

$$G_B^{T/2} = [1 + (FTF)^{T/2}(ITF)^{T/2} G_A^{T/2}[(JTF)^{T/6}(\frac{Az}{DE}\ ACT\ M_2)^{T/6}]^{T/2}]^{-1}(FTF)^{T/2} M_1^{T/2} \qquad (B\text{-}3)$$

$$G_C^T = (KTF)^T \qquad (B\text{-}4)$$

Equations B-2 and B-3 are first calculated and then substituted into Equation B-1. A complete numerical example is presented to help clarify each step in the evaluation process and to being the mathematical details sharply into focus.

MAJOR STEPS IN EVALUATION

The following transfer functions and sample rates are used in the scalar illustrative example:

$$(ATF)^{T/2} = (DTF)^{T/2} = (FTF)^{T/2} = \frac{T/4(z_2 + 1)}{(z_2 - 1)} \qquad (B\text{-}5)$$

$$(ITF)^{T/2} = (KTF)^{T} = 1.0 \tag{B-6}$$

$$(JTF)^{T/6} = \frac{z_6^2 + z_6 + 1}{3z_6^2} \tag{B-7}$$

$$\frac{q}{DE} = \frac{1}{s} \quad , \quad \frac{Az}{DE} = \frac{1}{s^2} \quad , \quad ACT = 1.0 \tag{B-8}$$

$$M_1 = \frac{1 - e^{-sT}}{s} \quad , \quad M_2 = \frac{1 - e^{-sT/2}}{s} \tag{B-9}$$

$$z_2 = e^{sT/2} \quad , \quad z_6 = e^{sT/6} \tag{B-10}$$

$$T = 1/40 \quad , \quad T/2 = 1/80 \quad , \quad T/6 = 1/240 \tag{B-11}$$

The evaluation of Equations B-1 through B-4 can be separated into nine major items. Each of these items require a series of numerical calculations. These major items are listed next.

(1) $[(JTF)^{T/6}(\frac{q}{DE}\ ACT\ M_2)^{T/6}]^{T/2}$

(2) $(ATF)^{T/2}(DTF)^{T/2}[(JTF)^{T/6}(\frac{q}{DE}\ ACT\ M_2)^{T/6}]^{T/2}$

(3) $[1 - (ATF)^{T/2}(DTF)^{T/2}[(JTF)^{T/6}(\frac{q}{DE}\ ACT\ M_2)^{T/6}]^{T/2}]^{-1}$

(4) $G_A^{T/2} = [1 - (ATF)^{T/2}(DTF)^{T/2}[(JTF)^{T/6}(\frac{q}{DE}\ ACT\ M_2)^{T/6}]^{T/2}]^{-1}(ATF)^{T/2}$

(5) $[(JTF)^{T/6}(\frac{Az}{DE}\ ACT\ M_2)^{T/6}]^{T/2}$

(6) $(FTF)^{T/2}(ITF)^{T/2}G_A^{T/2}[(JTF)^{T/6}(\frac{Az}{DE}\ ACT\ M_2)^{T/6}]^{T/2}$

(7) $[1 + (FTF)^{T/2}(ITF)^{T/2}G_A^{T/2}[(JTF)^{T/6}(\frac{Az}{DE}\ ACT\ M_2)^{T/6}]^{T/2}]^{-1}$

(8) $G_B^{T/2} = [1 + (FTF)^{T/2}(ITF)^{T/2}G_A^{T/2}[(JTF)^{T/6}(\frac{Az}{DE}\ ACT\ M_2)^{T/6}]^{T/2}]^{-1}(FTF)^{T/2}M_1^{T/2}$

(9) $\frac{A\dot{z}^T}{A\dot{z}_C^T} = [(\frac{Az}{DE}\ ACT\ M_2)^{T/2}G_A^{T/2}G_B^{T/2}]^T\ G_C^T$

In items 1, 5, and 9, a high-rate z-plane transfer function must be converted to an equivalent low-rate z-plane transfer function. For example, in item 1, the T/2 transform is obtained from a T/6 transform. That is,

$$[(JTF)^{T/6}(\frac{q}{DE}\ ACT\ M_2)^{T/6}]^{T/2} = [G_1^{T/6}(z_6)]^{T/2} = G_2^{T/2}(z_2) \qquad (B\text{-}12)$$

where

$$z_6 = e^{sT/6} \qquad (B\text{-}13)$$

and

$$z_2 = e^{sT/2} \qquad (B\text{-}14)$$

A number of techniques are available for calculating the standard z_6-transform of the s-plane function q/DE ACT M_2 [i.e., $(q/DE\ ACT\ M_2)^{T/6}$]. The most common technique is to apply partial fraction expansion to the s-plane function and then utilize a table of z-transform (Table 1). A computer program (ADVANZ) that implements this technique is described in Reference 11. The source listing for this program can be found in Reference 15 and is implemented as options 141-143 in TOTAL (Reference 13). This program converts a general s-plane transfer function into the z-, w-, or w'-plane. It can calculate the standard, delayed, or advanced discrete transform; and can insert a zero order, first order, second order, or

slewer data hold into the transformation.

The theoretical basis (and a computer program) for performing the high-to-low rate z-plane transform conversion in Equation B-12 is described in Reference 11. The source listing for this computer program (TXCONV) appears in Reference 15 and is implemented as options 144-149 in TOTAL. This program allows a high-rate transform in the z-, w-, or w'-plane to be converted to a low-rate discrete transform. The user simply inserts the high-rate transfer function $G_1^{T/6}$ and the sampling ratio (T/2)/(T/6) = 3 and the program calculates the low-rate transform $G_2^{T/2}$.

NUMERICAL CALCULATIONS

In this subsection, the actual numerical calculations for items 1-9 are carried out. It is normally necessary to utilize linear analysis software aids (e.g., TOTAL) to perform these calculations. However, the following calculations will be carried out essentially by hand.

ITEM 1 $[(JTF)^{T/6}(\frac{q}{DE}\ ACT\ M_2)^{T/6}]^{T/2}$

Substituting the appropriate transfer functions from Equations B-5 through B-9 produces

$$(\frac{q}{DE}\ ACT\ M_2)^{T/6} = (\frac{1 - e^{-sT/2}}{s}\ \frac{1}{s})^{T/6} \qquad (B\text{-}15)$$

Since $z_6 = e^{sT/6}$,

$$e^{-sT/2} = (e^{sT/6})^{-3} = z_6^{-3} \qquad (B\text{-}16)$$

Replacing $e^{-sT/2}$ in Equation B-15 with z_6^{-3} and pulling out the resulting z-plane factor gives

$$\left(\frac{q}{DE}\ \text{ACT}\ M_2\right)^{T/6} = (1 - z_6^{-3})\left(\frac{1}{s^2}\right)^{T/6} \qquad \text{(B-17)}$$

In Equation B-17, the T/6 z-transform of the s-plane transfer function $1/s^2$ is required. From a table of z-transforms (Table 1),

$$\left(\frac{q}{DE}\ \text{ACT}\ M_2\right)^{T/6} = (1 - z_6^{-3})\ \frac{(T/6)z_6}{(z_6 - 1)^2}$$

$$= \frac{(z_6 - 1)(z_6^2 + z_6 + 1)}{z_6^3}\ \frac{(T/6)z_6}{(z_6 - 1)^2} \qquad \text{(B-18)}$$

Then

$$\left[(JTF)^{T/6}\left(\frac{q}{DE}\ \text{ACT}\ M_2\right)^{T/6}\right]^{T/2} = \left[\frac{z_6^2 + z_6 + 1}{3z_6^2}\ \frac{(T/6)(z_6^2 + z_6 + 1)}{z_6^2(z_6 - 1)}\right]^{T/2}$$

$$= \left[\frac{(T/6)(z_6^2 + z_6 + 1)^2}{3z_6^4(z_6 - 1)}\right]^{T/2} \qquad \text{(B-19)}$$

The T/2 superscript notation in Equation B-19 tells us to take the $z_2 = e^{sT/2}$ transform of the function in the brackets. Since this function is a high-rate z-plane transfer function ($z_6 = e^{sT/6}$), a high-to-low transform conversion is needed. From Section III, Equation 71, this conversion can be obtained by combining the residues of the following expression.

$$G_2^{T/k}(z_k) = \left[G_1^{T/P}(z_p)\right]^{T/k} = \sum \text{residues}\ \frac{G_1^{T/p}(z_p)}{z_p}\ \frac{z_k}{z_k - z_p^N}\Bigg|_{z_p = \text{poles of } \frac{G_1^{T/p}(z_p)}{zp}} \qquad \text{(B-20)}$$

N = ratio of low-to-high rate sampling intervals (p/k)

$G_2^{T/k}(z_k)$ = low-rate z-plane function ($z_k = e^{sT/k}$)

$G_1^{T/P}(z_p)$ = high-rate z-plane function ($z_p = e^{sT/P}$)

For Equation B-19,

$$z_k = z_2 = e^{sT/2} \quad , \; z_p = z_6 = e^{sT/6} \quad , \; N = 3$$

and

$$\frac{G_1^{T/p}(z_p)}{z_p} = \frac{(JTF)^{T/6}(\frac{q}{DE}\ ACT\ M_2)^{T/6}}{z_p} = \frac{(T/6)(z_6^2 + z_6 + 1)^2}{3z_6^5(z_6 - 1)} \qquad (B\text{-}21)$$

Substituting Equation B-21 into Equation B-20 gives

$$[(JTF)^{T/6}(\frac{q}{DE}\ ACT\ M_2)^{T/6}]^{T/2} = \sum res\ \frac{(T/6)(z_6^2 + z_6 + 1)^2}{3z_6^5(z_6 - 1)}\ \frac{z_2}{z_2 - z_6^3}\Bigg|_{z_6 = 0,1} \qquad (B\text{-}22)$$

The residue calculations can be simplified by recognizing that $z_6^5 = z_6^3 z_6^2 = z_2 z_6^2$. The z_2 in the numerator of the $z_2/(z_2 - z_6^3)$ factor can then be cancelled and Equation B-22 reduces to

$$[(JTF)^{T/6}(\frac{q}{DE}\ ACT\ M_2)^{T/6}]^{T/2} = \frac{(T/6)}{3}\sum res\ \frac{(z_6^2 + z_6 + 1)^2}{z_6^2(z_6 - 1)(z_2 - z_6^3)}\Bigg|_{z_6 = 0,1} \qquad (B\text{-}23)$$

To calculate the residue at the $z_6 = 1$ pole, the $z_6 - 1$ factor is deleted and the remaining expression is evaluated at $z_6 = 1$.

$$\left.\frac{(z_6^2 + z_6 + 1)^2}{z_6^2(z_2 - z_6^3)}\right|_{z_6 = 1} = \frac{(1^2 + 1 + 1)^2}{1^2(z_2 - 1^3)} = \frac{9}{z_2 - 1} \qquad \text{(B-24)}$$

Since the pole at $z_6 = 0$ has a multiplicity of two (i.e., $z_6^2 = 0$), the first derivative of Equation B-23 must be obtained (with the z_6^2 pole deleted) before calculating the residue. That is,

$$\frac{d}{dz_6}\left[\frac{(z_6^2 + z_6 + 1)^2}{(z_6 - 1)(z_2 - z_6^3)}\right] z_6 = 0 \qquad \text{(B-25)}$$

or

$$\frac{d}{dz_6}\left[\frac{(z_6^2 + z_6 + 1)^2}{(z_6 z_2 - z_6^4 - z_2 + z_6^3)}\right] z_6 = 0 \qquad \text{(B-26)}$$

Taking the first derivative in Equation B-26 with respect to z_6 produces

$$\frac{(z_6 z_2 - z_6^4 - z_2 + z_6^3)\,[2(z_6^2 + z_6 + 1)(2z_6 + 1)] - (z_6^2 + z_6 + 1)^2(z_2 - 4z_6^3 + 3z_6^2)}{(z_6 z_2 - z_6^4 - z_2 + z_6^3)^2} \qquad \text{(B-27)}$$

The residue for the multiple pole at $z_6^2 = 0$ is obtained by evaluating Equation B-27 at $z_6 = 0$.

$$\frac{(-z_2)2(1)(1) - (1)^2(z_2)}{(-z_2)2} = \frac{-3}{z_2} \qquad \text{(B-28)}$$

Adding the residues from Equations B-24 and B-28 gives the desired low-rate z-plane transfer function for item 1.

$$(\text{ITEM 1}) = [(\text{JTF})^{T/6}(\frac{q}{DE}\ \text{ACT}\ M_2)^{T/6}]^{T/2} = (T/18)(\frac{9}{z_2 - 1} - \frac{3}{z_2})$$

$$= (T/18)\ \frac{6z_2 + 3}{z_2(z_2 - 1)} \qquad \text{(B-29)}$$

$$z_2 = e^{sT/2} \qquad \text{(B-30)}$$

ITEM 2 $\quad (\text{ATF})^{T/2}(\text{DTF})^{T/2}[(\text{JTF})^{T/6}(\frac{q}{DE}\ \text{ACT}\ M_2)^{T/6}]^{T/2}$

Substituting the appropriate transfer functions from Equation B-5 and the transfer function in Equation B-29 gives

$$(\text{ITEM 2}) = (T/4)\ \frac{z_2 + 1}{z_2 - 1}\ (T/4)\ \frac{z_2 + 1}{z_2 - 1}\ (T/18)\ \frac{6z_2 + 3}{z_2(z_2 - 1)}$$

$$= K\ \frac{(z_2 + 1)^2(6z_2 + 3)}{z_2(z_2 - 1)^3} \qquad \text{(B-31)}$$

where

$$K = T^3/(16)(18) \qquad \text{(B-32)}$$

ITEM 3 $\quad [1 - (\text{ATF})^{T/2}(\text{DTF})^{T/2}[(\text{JTF})^{T/6}(\frac{q}{DE}\ \text{ACT}\ M_2)^{T/6}]^{T/2}]^{-1}$

Substituting, the inverse becomes

$$(\text{ITEM 3}) = [1 - K\ \frac{(z_2 + 1)^2(6z_2 + 3)}{z_2(z_2 - 1)^3}]^{-1}$$

$$= \left[\frac{z_2(z_2 - 1)^3 - K\,(z_2 + 1)^2(6z_2 + 3)}{z_2(z_2 - 1)^3}\right]^{-1}$$

$$= \frac{z_2(z_2 - 1)^3}{z_2^4 - (3 + 6K)z_2^3 + (3 - 15K)z_2^2 - (1 + 12K)z_2 - 3K} \qquad \text{(B-33)}$$

ITEM 4 $G_A^{T/2} = [1 - (ATF)^{T/2}(DTF)^{T/2}[(JTF)^{T/6}(\frac{q}{DE}\ ACT\ M_2)^{T/6}]^{T/2}]^{-1}(ATF)^{T/2}$

Substituting for filter $(ATF)^{T/2}$ and utilizing Equation B-33, item 4 is given by

$$(ITEM\ 4) = \frac{(T/4)z_2(z_2 - 1)^2(z_2 + 1)}{z_2^4 - (3 + 6K)z_2^3 + (3 - 15K)z_2^2 - (1 + 12K)z_2 - 3K} \qquad \text{(B-34)}$$

ITEM 5 $[(JTF)^{T/6}(\frac{Az}{DE}\ ACT\ M_2)^{T/6}]^{T/2}$

Using the same procedures as for item 1 results in the following:

$$(\frac{Az}{DE}\ ACT\ M_2)^{T/6} = (\frac{1 - e^{-sT/2}}{s}\frac{1}{s^2})^{T/6}$$

$$= (1 - z_6^{-3})(\frac{1}{s^3})^{T/6} = \frac{z_6^3 - 1}{z_6^3}\ \frac{(T/6)^2 z_6(z_6 + 1)}{2(z_6 - 1)^3}$$

$$= \frac{(z_6 - 1)(z_6^2 + z_6 + 1)}{z_6^3}\ \frac{(T/6)^2 z_6(z_6 + 1)}{2(z_6 - 1)^3}$$

$$= K_1 \frac{(z_6^2 + z_6 + 1)(z_6 + 1)}{z_6^2(z_6 - 1)^2} \tag{B-35}$$

where

$$K_1 = (T/6)^2/2 \tag{B-36}$$

Then

$$[(JTF)^{T/6}(\frac{Az}{DE} \text{ ACT } M_2)^{T/6}]^{T/2} = [\frac{z_6^2 + z_6 + 1}{3z_6^2} \quad K_1 \frac{(z_6^2 + z_6 + 1)(z_6 + 1)}{z_6^2(z_6 - 1)^2}]^{T/2}$$

$$= K_2 [\frac{(z_6^2 + z_6 + 1)^2(z_6 + 1)}{z_6^4(z_6 - 1)^2}]^{T/2} \tag{B-37}$$

In Equation B-37,

$$K_2 = K_1/3 = (T/6)^2/6 \tag{B-38}$$

The next step is to substitute Equation B-37 into Equation B-20 and evaluate the residues associated with the poles at $z_6 = 0$ and $z_6 = 1$.

$$(\text{ITEM 5}) = K_2 \sum \text{residues} \frac{(z_6^2 + z_6 + 1)^2(z_6 + 1)}{z_6^5(z_6 - 1)^2} \frac{z_2}{z_2 - z_6^3} \Bigg|_{z_6 = 0,1} \tag{B-39}$$

Again recognizing that $z_6^5 = z_2 z_6^2$, Equation B-39 can be simplified to

$$(\text{ITEM 5}) = K_2 \sum \text{residues} \left. \frac{(z_6^2 + z_6 + 1)^2 (z_6 + 1)}{z_6^2 (z_6 - 1)^2 (z_2 - z_6^3)} \right|_{z_6 = 0,1} \tag{B-40}$$

The residue associated with the pole at $z_6^2 = 0$ is given by

$$\frac{d}{dz_6} \left[\frac{(z_6^2 + z_6 + 1)^2 (z_6 + 1)}{(z_6 - 1)^2 (z_2 - z_6^3)} \right] \Bigg|_{z_6 = 0} = \frac{5}{z_2} \tag{B-41}$$

In a like manner, the residue for the $z_6 = 1$ pole is given by

$$\frac{d}{dz_6} \left[\frac{(z_6^2 + z_6 + 1)^2 (z_6 + 1)}{z_6^2 (z_2 - z_6^3)} \right] \Bigg|_{z_6 = 1} = \frac{9(z_2 + 5)}{(z_2 - 1)^2} \tag{B-42}$$

The low-rate z-plane transfer function form item 5 is obtained by adding the residues in Equations B-41 and B-42.

$$(\text{ITEM 5}) = K_2 \left[\frac{5}{z_2} + \frac{9(z_2 + 5)}{(z_2 - 1)^2} \right] = K_2 \frac{14 z_2^2 + 35 z_2 + 5}{z_2 (z_2 - 1)^2} \tag{B-43}$$

<u>ITEM 6</u> $(\text{FTF})^{T/2} (\text{ITF})^{T/2} G_A^{T/2} [(\text{JTF})^{T/6} (\frac{Az}{DE} \text{ ACT } M_3)^{T/6}]^{T/2}$

Substituting Equations B-5, B-6, B-34, and B-43 into item 6 produces

$$(\text{ITEM 6}) = (T/4)\ \frac{z_2 + 1}{z_2 - 1}\ \frac{(T/4)z_2(z_2 - 1)^2(z_2 + 1)}{z_2^4 - (3 + 6K)z_2^3 + (3 - 15K)z_2^2 - (1 + 12K)z_2 - 3K}$$

$$* K_2\ \frac{14z_2^2 + 35z_2 + 5}{z_2(z_2 - 1)^2}$$

$$= K_3\ \frac{(z_2 + 1)^2(14z_2^2 + 35z_2 + 5)}{(z_2 - 1)\ [z_2^4 - (3 + 6K)z_2^3 + (3 - 15K)z_2^2 - (1 + 12K)z_2 - 3K]} \qquad \text{(B-44)}$$

where

$$K_3 = (T/4)^2K_2 = (T/4)^2(T/6)^2/6 \qquad \text{(B-45)}$$

ITEM 7 $[1 + (FTF)^{T/2}(ITF)^{T/2}G_A^{T/2}[(JTF)^{T/6}(\frac{Az}{DE}\ ACT\ M_2)^{T/6}]^{T/2}]^{-1}$

Utilizing Equation B-44, the inverse in item 7 is given by

$$(\text{ITEM 7}) = \left[1 + K_3\ \frac{(z_2 + 1)^2(14z_2^2 + 35z_2 + 5)}{(z_2 - 1)[z_2^4 - (3 + 6K)z_2^3 + (3 - 15K)z_2^2 - (1 + 12K)z_2 - 3K]}\right]^{-1}$$

$$= \frac{(z_2 - 1)(z_2^4 + a_3z_2^3 + a_2z_2^2 + a_1z_2 + a_0)}{z_2^5 + b_4z_2^4 + b_3z_2^3 + b_2z_2^2 + b_1z_2 + b_0} \qquad \text{(B-46)}$$

where

$$b_4 = -(4 + 6K - 14K_3) \qquad a_3 = -(3 + 6K)$$

$$b_3 = (6 - 9K + 63K_3) \qquad a_2 = (3 - 15K)$$

$$b_2 = -(4 - 3K - 89K_3) \qquad a_1 = -(1 + 12K)$$

$$b_1 = (1 + 9K + 45K_3) \qquad a_0 = -(3K)$$

$$b_0 = (3K + 5K_3)$$

$$K = T^3/(16)(18) \qquad K_3 = (T/4)^2(T/6)^2/6$$

ITEM 8 $$G_B^{T/2} = [1 + (FTF)^{T/2}(ITF)^{T/2}G_A^{T/2}[(JTF)^{T/6}(\frac{Az}{DE}\ ACT\ M_2)^{T/6}]^{T/2}]^{-1}$$

$$* (FTF)^{T/2}M_1^{T/2}$$

Before forming $G_B^{T/2}$, the transform $M_1^{T/2}$ must be calculated. From Equation B-9 we have

$$M_1^{T/2} = (\frac{1 - e^{-sT}}{s})^{T/2} = (1 - z^{-2}_2)(\frac{1}{s})^{T/2}$$

$$= \frac{z_2^2 - 1}{z_2^2} \frac{z_2}{z_2 - 1} = \frac{z_2 + 1}{z_2} \qquad (B-47)$$

Combining Equations B-46 and B-47 with the $(FTF)^{T/2}$ filter in Equation B-5 gives

$$(ITEM\ 8) = G_B^{T/2} = \frac{(T/4)(z_2 + 1)^2(z_2^4 + a_3z_2^3 + a_2z_2^2 + a_1z_2 + a_0)}{z_2(z_2^5 + b_4z_2^4 + b_3z_2^3 + b_2z_2^2 + b_1z_2 + b_0)}$$

ITEM 9 $$\frac{A\overset{T}{z}}{A\overset{T}{z}_C} = [(\frac{Az}{DE}\ ACT\ M_2)^{T/2}G_A^{T/2}G_B^{T/2}]^T\ G_C^T$$

The s-plane to z-plane transform in item 9 is given by

$$(\frac{Az}{DE}\ ACT\ M_2)^{T/2} = (\frac{1 - e^{-sT/2}}{s}\ \frac{1}{s^2})^{T/2}$$

$$= (1 - z_2^{-1})\left(\frac{1}{s^3}\right)^{T/2}$$

$$= \frac{z_2 - 1}{z_2} \; \frac{(T/2)^2 z_2(z_2 + 1)}{2(z_2 - 1)^3}$$

$$= \frac{(T^2/8)(z_2 + 1)}{(z_2 - 1)^2} \qquad \text{(B-48)}$$

And

$$\frac{A\hat{z}^T}{A\hat{z}_C^T} = \left[\frac{(T^2/8)(z_2 + 1)}{(z_2 - 1)^2} \; \frac{(T/4)z_2(z_2 - 1)^2(z_2 + 1)}{(z_2^4 + a_3z_2^3 + a_2z_2^2 + a_1z_2 + a_0)}\right.$$

$$\left. * \frac{(T/4)(z_2 + 1)^2(z_2^4 + a_3z_2^3 + a_2z_2^2 + a_1z_2 + a_0)}{z_2(z_2^5 + b_4z_2^4 + b_3z_2^3 + b_2z_2^2 + b_1z_2 + b_0)} \; \frac{1}{1}\right]^T$$

$$= \left[\frac{(T^4/128)(z_2 + 1)^4}{(z_2^5 + b_4z_2^4 + b_3z_2^3 + b_2z_2^2 + b_1z_2 + b_0)}\right]^T \qquad \text{(B-49)}$$

The evaluation of the high-to-low rate transform conversion in Equation B-49 is tedious. The results of applying option 149 of TOTAL is shown below.

$$\frac{A\hat{z}^T}{A\hat{z}_C^T} = \frac{(-.8024E\text{-}13)z^5 + (.2441E\text{-}07)z^4 + (.1709E\text{-}06)z^3 + (.1709E\text{-}06)z^2 + (.2441E\text{-}07)z - (.9968E\text{-}15)}{(1.000)z^5 - (4.000)z^4 + (6.000)z^3 - (4.000)z^2 + (1.000)z - (.2667E\text{-}13)} \qquad \text{(B-50)}$$

Equation B-50 is the desired closed-loop z-plane transfer function defined for $z = e^{sT}$.

APPENDIX C

MECHANIZATION OF MULTI-RATE MODEL EQUATIONS USING TOTAL

INTRODUCTION

An automated technique for evaluating multi-rate model equations is presented. This technique employs the transfer function storage and macro options in the linear analysis computer program TOTAL (Reference 13). The closed-loop multi-rate model equation in Section V (Equation 103) is used to illustrate this technique. Equation 103 is repeated below as Equation C-1.

$$\frac{A_z^T}{A_{z_C}^T} = \left[\left(\frac{Az}{DE}\ ACT\ M_2\right)^{T/2} G_A^{T/2} G_B^{T/2}\right]^T G_C^T \qquad (C\text{-}1)$$

In Equation C-1, the following definitions apply (see Equations 104-106)

$$G_A^{T/2} = \left[1 - (ATF)^{T/2}(DTF)^{T/2}\left[(JTF)^{T/6}\left(\frac{q}{DE}\ ACT\ M_2\right)^{T/6}\right]^{T/2}\right]^{-1} (ATF)^{T/2} \qquad (C\text{-}2)$$

$$G_B^{T/2} = \left[1 + (FTF)^{T/2}(ITF)^{T/2} G_A^{T/2}\left[(JTF)^{T/6}\left(\frac{Az}{DE}\ ACT\ M_2\right)^{T/6}\right]^{T/2}\right]^{-1}$$

$$* \quad (FTF)^{T/2} M_1^{T/2} \qquad (C\text{-}3)$$

$$G_C^T = (KTF)^T \qquad (C\text{-}4)$$

To apply this automated technique, the s-plane and z-plane transfer functions that appear in Equations C-1 through C-4 are stored in TOTAL. A user generated macro is then executed that accesses these transfer functions and performs a sequence of operations to solve the multi-rate equation. The transfer function storage and macro capabilities of TOTAL are described in the following subsections.

TRANSFER FUNCTION STORAGE

TOTAL has 24 auxiliary transfer function storage locations designated by ATF, BTF, ... , ZTF (GTF and HTF serve other functions within the program and are excluded from this list). This specific transfer function notation is used in the multi-rate model equations. However, in Equations C-1 through C-4, storage locations must also be assigned to $M_1^{T/2}$, M_2, ACT, q/DE, and AZ/DE.

In Equation C-3, $M_1^{T/2}$ is defined by

$$M_1^{T/2} = \left(\frac{1 - e^{-sT}}{s}\right)^{T/2} \qquad \text{(C-5)}$$

To evaluate Equation C-5, the z-plane factor is pulled out and the T/2 transform is obtained for the remaining s-plane factor. That is,

$$M_1^{T/2} = (1 - z_2^{-2})\left(\frac{1}{s}\right)^{T/2}$$

$$= \frac{z_2^2 - 1}{z_2} \; \frac{z_2}{z_2 - 1}$$

$$= \frac{z_2 + 1}{z_2} \qquad \text{(C-6)}$$

where

$$z_2 = e^{sT/2} \qquad \text{(C-7)}$$

For the macro calculations, we let

$$M_1^{T/2} = (\text{LTF})^{T/2} = \frac{z_2 + 1}{z_2} \qquad \text{(C-8)}$$

The M_2 data hold appears in the following three transforms:

$$\left(\frac{Az}{DE}\ ACT\ M_2\right)^{T/2} \tag{C-9}$$

$$\left(\frac{q}{DE}\ ACT\ M_2\right)^{T/6} \tag{C-10}$$

$$\left(\frac{Az}{DE}\ ACT\ M_2\right)^{T/6} \tag{C-11}$$

In Equation C-9, it is not necessary to explicitly store M_2 in TOTAL to calculate the T/2 s-plane to z-plane transform. Since M_2 is referenced to a T/2 sampling interval ($M_2 = 1 - e^{-sT/2}/s$), option 141 in TOTAL will insert M_2 before taking the transform. The user simply supplies the Az/DE and ACT s-plane transfer functions.

The above simplification for the M_2 data hold is not possible in Equations C-10 and C-11 since the sampling interval is T/6. It will be necessary to separate M_2 into z-plane and s-plane factors and place each in a separate transfer function storage location. Substituting for M_2, Equations C-10 and C-11 become

$$\left(\frac{q}{DE}\ ACT\ M_2\right)^{T/6} = \left(\frac{q}{DE}\ ACT\ \frac{1 - e^{-sT/2}}{s}\right)^{T/6}$$

$$= \frac{z_6^3 - 1}{z_6^3}\left(\frac{q}{DE}\ ACT\ \frac{1}{s}\right)^{T/6} \tag{C-12}$$

$$\left(\frac{Az}{DE}\ ACT\ M_2\right)^{T/6} = \left(\frac{Az}{DE}\ ACT\ \frac{1 - e^{-sT/2}}{s}\right)^{T/6}$$

$$= \frac{z_6^3 - 1}{z_6^3}\left(\frac{Az}{DE}\ ACT\ \frac{1}{s}\right)^{T/6} \tag{C-13}$$

where

$$z_6 = e^{sT/6} \tag{C-14}$$

For the macro, the z-plane and s-plane factors in Equations C-12 and C-13 will be stored as

$$(\text{MTF})^{T/6} = \frac{z_6^3 - 1}{z_6^3} \tag{C-15}$$

$$\text{NTF} = \frac{1}{s} \tag{C-16}$$

The remaining transfer function storage allocations are given below.

$$\text{BTF} = \text{ACT} \tag{C-17}$$

$$\text{CTF} = \frac{q}{DE} \tag{C-18}$$

$$\text{ETF} = \frac{Az}{DE} \tag{C-19}$$

$$\text{YTF} = \frac{1}{1} \tag{C-20}$$

$$\text{ZTF} = \frac{-1}{1} \tag{C-21}$$

The unity transfer functions YTF and ZTF are needed in the macro to perform the inverse calculations.

Utilizing the above storage allocations for $M_1^{T/2}$, M_2, ACT, q/DE, and Az/DE, Equations C-1 through C-4 can be expressed as

$$\begin{matrix} \overset{T}{\frac{Az}{}} \\ \underset{C}{Az^T} \end{matrix} = [(\text{ETF BTF } M_2)^{T/2} G_A^{T/2} G_B^{T/2}]^T \; G_C^T \tag{C-22}$$

$$G_A^{T/2} = [1 - (\text{ATF})^{T/2}(\text{DTF})^{T/2}[(\text{JTF})^{T/6}(\text{MTF})^{T/6}(\text{CTF BTF NTF})^{T/6}]^{T/2}]^{-1}$$

$$* \ (ATF)^{T/2} \tag{C-23}$$

$$G_B^{T/2} = [1 + (FTF)^{T/2}(ITF)^{T/2}G_A^{T/2}[(JTF)^{T/6}(MTF)^{T/6}(ETF\ BTF\ NTF)^{T/6}]^{T/2}]^{-1}$$

$$* \ (FTF)^{T/2}(LTF)^{T/2} \tag{C-24}$$

$$G_C^T = (KTF)^T \tag{C-25}$$

As pointed out, it is not necessary to store the M_2 transfer function that appears in Equation C-22. It will be inserted by option 141 in TOTAL before the T/2 s-plane to z_2-plane transformation is calculated.

MACRO INSTRUCTION SET

The macro capability of the TOTAL computer program can be used to perform the series of operations in Equations C-22 through C-25. A macro operates as an executive instruction set for TOTAL. Each macro contains up to 98 sequential instructions. Typical instructions include the following: (1) copy a transfer function from one storage location to another, (2) multiply or add two transfer functions, (3) set an internal variable to a numerical value, (4) set a logic switch to true or false, (5) perform a s-plane to z-plane transformation, and (6) calculate a low-rate z-plane transfer function from a given high-rate z-plane transfer function. These instructions represent a small sample of the large number of options available in TOTAL (there are over 100 active options).

The first step in evaluating the multi-rate equations is to sequentially list the necessary individual operations. Each operation is then related to a specific series of commands and options in TOTAL. Finally, by invoking the special CREATE command in TOTAL, this sequential list of commands and

options is converted to a coded macro instruction set.

The AKEY, BKEY, and CKEY macros for Equations C-22 through C-25 are given in Tables C-1, C-2, and C-3. Column one in these tables sequentially lists the individual operations, and column two lists the corresponding TOTAL commands and options. The sampling intervals used in these macros are T = 1/40, T/2 = 1/80, and T/6 = 1/240. Table C-4 outlines the specific TOTAL commands and options utilized in the macros.

As specified by the user, TOTAL stores the coded macro instructions in local files AKEY, BKEY, or CKEY. These local files can be cataloged as permanent files for future use. For Equations C-22 through C-25, it is necessary to divide the instructions between the three macros. Each macro is limited to 98 instructions, and 232 instructions are required to evaluate these multi-rate equations. The AKEY macro contains 93 instructions, BKEY 85 instructions, and CKEY 54 instructions.

It is the users responsibility to keep track of the instruction count. In each macro, a complete copy operation takes three instructions (e.g., COPY, NTF, GTF); setting a variable to a numerical values also takes three instructions (e.g., TSAMP = .004167); and an option number requires one instruction (e.g., 21, 24, 141, or 149).

To execute the AKEY macro in TOTAL, the command AKEY is given while in the option mode. That is,

OPTION > AKEY

TOTAL will then go to the local file AKEY and read and execute each instruction in a sequential fashion. From Table C-1, the first three instructions will copy the transfer function stored in NTF into the GTF storage location.

Following this, TOTAL will copy the contents of BTF into HTF. Option 21 will next multiply GTF and HTF and store the resulting transfer function in OLTF. The last instruction in AKEY is to call BKEY. When TOTAL encounters this command, it immediately begins to read the instructions in the local file BKEY. In a similar manner, the last instruction in the BKEY macro is to call the CKEY macro.

TABLE C-1. AKEY MACRO - $G_A^{T/2}$

OPERATION	COMMAND/OPTION
BTF NTF	COPY, NTF, GTF COPY, BTF, HTF 21
CTF BTF NTF	COPY, OLTF, GTF COPY, CTF, HTF 21
$G_1^{T/6} = (CTF\ BTF\ NTF)^{T/6}$	COPY, OLTF, CLTF TSAMP=.004167 HOLD=4 DELTA=0 141
$(MTF)^{T/6}G_1^{T/6}$	COPY, CLTF, GTF COPY, MTF, HTF 21
$(JTF)^{T/6}(MTF)^{T/6}G_1^{T/6}$	COPY, OLTF, GTF COPY, JTF, HTF 21
$G_2^{T/2} = [(JTF)^{T/6}(MTF)^{T/6}G_1^{T/6}]^{T/2}$	COPY, OLTF, CLTF HISAMP=1.0 LOSAMP=3.0 149
$(DTF)^{T/2}G_2^{T/2}$	COPY, CLTF, GTF COPY, DTF, HTF 21
$G_3^{T/2} = (ATF)^{T/2}(DTF)^{T/2}G_2^{T/2}$	COPY, OLTF, GTF COPY, ATF, HTF 21
$-G_3^{T/2}$	COPY, OLTF, GTF COPY, ZTF, HTF 21
$I - G_3^{T/2}$	COPY, OLTF, GTF COPY, YTF, HTF 24
$(I - G_3^{T/2})^{-1}$	COPY, CLNPOLY, GDPOLY COPY, CLDPOLY, GNPOLY
$G_A^{T/2} = (I - G_3^{T/2})^{-1}(ATF)^{T/2}$	COPY, ATF, HTF 21
STORE $G_A^{T/2}$ IN OTF	COPY, OLTF, OTF
CALL BKEY	BKEY

TABLE C-2. BKEY - $G_B^{T/2}$

OPERATION	COMMAND/OPTION
BTF NTF	COPY, NTF, GTF COPY, BTF, HTF 21
ETF BTF NTF	COPY, OLTF, GTF COPY, ETF, HTF 21
$G_1^{T/6} = (\text{ETF BTF NTF})^{T/6}$	COPY, OLTF, CLTF 141
$(\text{MTF})^{T/6} G_1^{T/6}$	COPY, CLTF, GTF COPY, MTF, HTF 21
$(\text{JTF})^{T/6} (\text{MTF})^{T/6} G_1^{T/6}$	COPY, OLTF, GTF COPY, JTF, HTF 21
$G_2^{T/2} = [(\text{JTF})^{T/6} (\text{MTF})^{T/6} G_1^{T/6}]^{T/2}$	COPY, OLTF, CLTF 149
$G_A^{T/2} G_2^{T/2}$	COPY, CLTF, GTF COPY, OTF, HTF 21
$(\text{ITF})^{T/2} G_A^{T/2} G_2^{T/2}$	COPY, OLTF, GTF COPY, ITF, HTF 21
$G_3^{T/2} = (\text{FTF})^{T/2} (\text{ITF})^{T/2} G_A^{T/2} G_2^{T/2}$	COPY, OLTF, GTF COPY, FTF, HTF 21
$I + G_3^{T/2}$	COPY, OLTF, GTF COPY, YTF, HTF 24
$(I + G_3^{T/2})^{-1}$	COPY, CLNPOLY, GDPOLY COPY, CLDPOLY, GNPOLY
$(I + G_3^{T/2})^{-1} (\text{FTF})^{T/2}$	COPY, FTF, HTF 21
$G_B^{T/2} = (I + G_3^{T/2})^{-1} (\text{FTF})^{T/2} (\text{LTF})^{T/2}$	COPY, OLTF, GTF COPY, LTF, HTF 21
STORE $G_B^{T/2}$ IN PTF	COPY, OLTF, PTF
CALL CKEY	CKEY

AD-A152 044 MULTI-RATE DIGITAL AUTOPILOT MODELING METHODOLOGY(U) 2/2
ARMAMENT DIV (AFSC) EGLIN AFB FL D G DIDALEUSKY MAR 85
AD-TR-83-64 AFATL-TR-83-67

UNCLASSIFIED F/G 1/3 NL

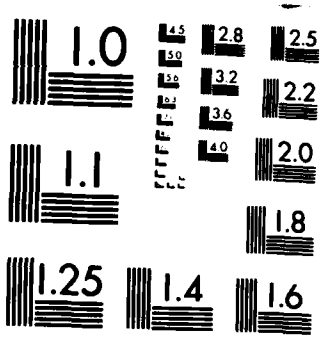

MICROCOPY RESOLUTION TEST CHART
NATIONAL BUREAU OF STANDARDS-1963-A

TABLE C-3. CKEY MACRO - $A\ddot{z}^T/A\ddot{z}_C^T$

OPERATION	COMMAND/OPTION
ETF BTF	COPY, BTF, GTF COPY, ETF, HTF 21
$G_1^T/2 = (ETF\ BTF\ M_2)^{T/2}$	COPY, OLTF, CLTF TSAMP=.0125 HOLD=0 DELTA=0 141
$G_1^T/2 G_A^T/2$	COPY, CLTF, GTF COPY, OTF, HTF 21
$G_1^T/2 G_A^T/2 G_B^T/2$	COPY, OLTF, GTF COPY, PTF, HTF 21
$(G_1^T/2 G_A^T/2 G_B^T/2)^T$	COPY, OLTF, CLTF HISAMP=1.0 LOSAMP=2.0 149
$\frac{A\ddot{z}^T}{A\ddot{z}_C^T} = (G_1^T/2 G_A^T/2 G_B^T/2)^T G_C^T$	COPY, CLTF, GTF COPY, KTF, HTF 21
STORE $A\ddot{z}^T/A\ddot{z}_C^T$ IN QTF	COPY, OLTF, QTF

TABLE C-4. TOTAL COMMANDS AND OPTIONS

COMMANDS/OPTIONS	DESCRIPTION
COPY, NTF, GTF	Copies transfer function stored in NTF into storage location GTF. Leaves contents of NTF unaltered.
21	Option 21. OLTF = GTF * HTF Multiplies transfer functions stored in GTF and HTF and stores product in OLTF.
24	Option 24. CLTF = GTF + HTF Adds transfer functions stored in GTF and HTF and stores sum in CLTF.
141	Option 141. Converts s-plane transfer function stored in CLTF to z-plane transfer function and stores results in CLTF.
TSAMP	Sampling interval (sec).
HOLD	Hold option: (0) zero-order, (1) first-order, (2) second-order, (3) slewer, or (4) none.
DELTA	Transform option: (0) standard transform, (+) advanced transform, or (-) delayed transform.
149	Option 149. Converts high-rate z-plane transfer function stored in CLTF to low-rate z-plane transfer function. Stores results in CLTF.
HISAMP	High rate sampling interval.
LOSAMP	Low rate sampling interval (Only ratio of sampling intervals needed for HISAMP and LOSAMP.)

INITIAL DISTRIBUTION

DTIC-DDAC	2
AUL/LSE	1
FTD/SDNF	1
HQ USAFE/INAT	1
AFWAL (FIES/CDIC)	1
AFWAL (FIGL)	2
COMDR NAVAIRSYSCOMD (CODE AIR-5401E)	10
AD/ENMA	10
AD/YMEB	3
AD/XRCD	1
AFATL/DLMA	2
LEAR SIEGLER, INC.	1
GEN ELECTRIC COMPANY	1
BOEING AEROSPACE COMPANY	1
NORTHROP CORPORATION	1
WRIGHT STATE UNIVERSITY	1
AFALT/DLODL	2

(The reverse of this page is blank.)

END

FILMED

4-85

DTIC